Review

Not peer-reviewed version

Advanced TiO_2-Based Photoelectrocatalysis: Material Modifications, Charge Dynamics, and Environmental–Energy Applications

Xiongwei Liang , Shaopeng Yu * , Bo Meng , Xiaodi Wang , Chunxue Yang , Chuanqi Shi , Junnan Ding

Posted Date: 15 April 2025

doi: 10.20944/preprints202504.1178.v1

Keywords: TiO_2 photoelectrocatalysis; Visible light response; Metal doping; Water purification; Reactive oxygen species; Charge separation

Preprints.org (www.preprints.org) | NOT PEER-REVIEWED | Posted: 15 April 2025 doi:10.20944/preprints202504.1178.v1

Review

Advanced TiO_2-Based Photoelectrocatalysis: Material Modifications, Charge Dynamics, and Environmental–Energy Applications

Xiongwei Liang [1,2], Shaopeng Yu [1,*], Bo Meng [1,2], Xiaodi Wang [1], Chunxue Yang [1,2], Chuanqi Shi [1] and Junnan Ding [1]

[1] Cold Region Wetland Ecology and Environment Research Key Laboratory of Heilongjiang Province, Harbin University; 150086, China. liangxiongwei007@163.com (X.L.) ; mengbomune@aliyun.com (B.M.) ; yayawxd123@126.com (X.W.) ; yangchunxue1984@163.com (C.Y.) ; chuanqi0730@163.com (C.S.) ; ding.junnan@163.com (J.D.)
[2] State Key Laboratory of Urban Water Resource and Environment, Harbin Institute of Technology, 150086, China.
* Correspondence: shaopengyu1972@163.com

Abstract: This review presents a comprehensive overview of recent advances in TiO_2-based photoelectrocatalysis (PEC) , with an emphasis on material design strategies to enhance visible-light responsiveness and charge carrier dynamics. Key approaches—including elemental doping, defect engineering, heterojunction construction, and plasmonic enhancement—are systematically discussed in relation to their roles in modulating energy band structures and promoting charge separation. Beyond fundamental mechanisms, the review highlights the broad environmental and energy-related applications of TiO_2-driven PEC systems, encompassing the degradation of persistent organic pollutants, microbial disinfection, heavy metal removal, photoelectrochemical water splitting for hydrogen production, and CO_2 reduction. Recent progress in integrating PEC systems with energy harvesting modules to construct self-powered platforms is critically examined. Current limitations and future directions are also outlined to guide the rational development of next-generation TiO_2-based photoelectrocatalytic systems for sustainable environmental remediation and solar fuel conversion.

Keywords: TiO_2 photoelectrocatalysis; Visible light response; Metal doping; Water purification; Reactive oxygen species；Charge separation

1. Introduction

Water pollution arising from organic contaminants released via agricultural runoff, industrial effluents, and diverse anthropogenic activities has become a pressing global environmental concern over recent decades. Many of these pollutants are classified as emerging contaminants, notable for their persistence in aquatic environments and resistance to degradation by conventional wastewater treatment processes. Such recalcitrant substances—including synthetic chemicals, industrial dyes, pharmaceutical residues, and agrochemicals like pesticides—pose significant ecological and public health risks due to their established toxicity, mutagenicity, and carcinogenic potential [1–5]. Notably, approximately 300,000 tons of dye-contaminated effluents from textile industries are annually discharged into water bodies worldwide, significantly deteriorating water quality and adversely impacting aquatic biodiversity [5,6].

Conventional wastewater treatments, comprising biological, physicochemical, and chemical methods, have demonstrated limited efficacy in eliminating persistent organic pollutants (POPs) , primarily due to these compounds' inherent chemical stability and low biodegradability [7–13]. In addressing this challenge, advanced oxidation processes (AOPs) have emerged as a promising alternative, utilizing highly reactive species to effectively degrade recalcitrant contaminants [14–16].

Among various AOPs, photoelectrocatalysis (PEC) has attracted considerable scientific attention due to its superior efficiency compared to traditional photocatalysis. PEC synergistically combines photocatalytic and electrochemical oxidation mechanisms, overcoming limitations inherent in the standalone applications of each method [17–19]. This growing interest in PEC is reflected in the sharp increase in scientific publications over the past two decades, as illustrated in Figure 1.

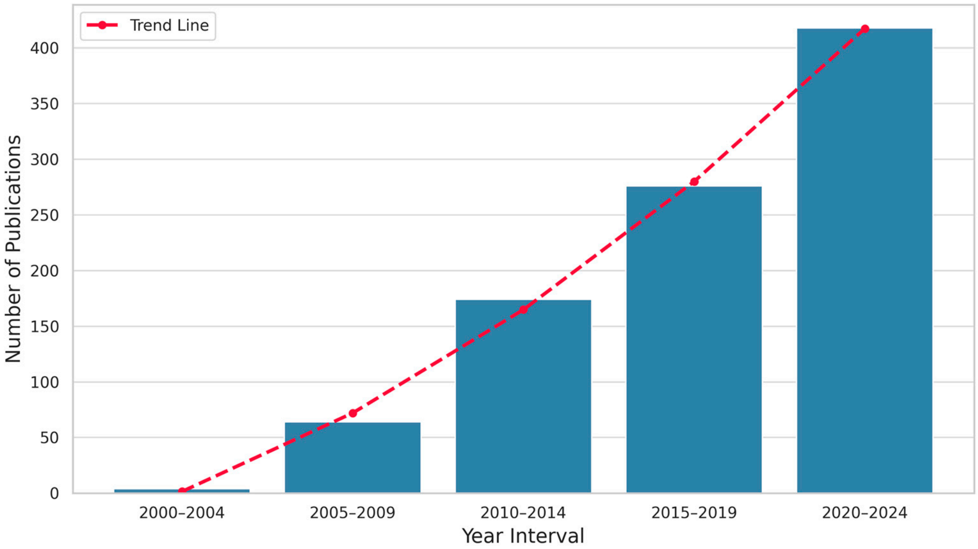

Figure 1. Publication trends on photoelectrocatalysis (PEC) for environmental remediation, categorized by 5-year intervals from 2000 to 2024. Data obtained from Web of Science Collection using keywords: "photoelectrocatalysis" AND "TiO_2".

In PEC, an external bias voltage is applied across a semiconductor-based photocatalyst immobilized on a conductive substrate. Illumination with photons of energy equal to or greater than the semiconductor's bandgap results in the excitation of electrons from the valence to the conduction band, generating electron–hole pairs. The external bias promotes rapid separation of these charge carriers, directing electrons toward the cathode and holes toward the photoanode interface, thus effectively mitigating recombination—a significant limitation of conventional photocatalysis—and enhancing quantum efficiency and degradation performance [20–22].

Among the semiconductor materials explored, titanium dioxide (TiO_2) stands out as the most extensively investigated due to its exceptional intrinsic photocatalytic activity, chemical and thermal stability, environmental friendliness, resistance to photocorrosion, and cost-effectiveness [23–25]. Since Fujishima and Honda first demonstrated TiO_2-based photoelectrochemical water splitting in 1972 [21], TiO_2 has been extensively studied for diverse environmental applications, including water and air purification and solar energy conversion.

Nevertheless, pristine TiO_2 exhibits critical limitations hindering practical application, notably its wide bandgap (3.0–3.2 eV) , restricting optical absorption primarily to the ultraviolet region (~5% of the solar spectrum) , and a high recombination rate of photogenerated electron–hole pairs, significantly reducing quantum efficiency [26–28]. These intrinsic drawbacks have prompted substantial research into modifying TiO_2 to enhance visible light absorption and improve charge carrier dynamics.

Numerous strategies have emerged to address these limitations, including elemental doping (with metals and non-metals) , defect engineering, heterojunction design, and exploitation of surface plasmon resonance (SPR) effects [29–32]. These approaches aim to modify the electronic structure of TiO_2, narrowing its bandgap, extending absorption to visible wavelengths, and enhancing charge separation and carrier transport. Advances in nanomaterial synthesis and cutting-edge characterization techniques have accelerated the development of advanced TiO_2-based PEC systems with improved visible-light-driven performance [33,34].

The application of TiO_2-based PEC systems in environmental remediation has demonstrated substantial potential, effectively degrading diverse organic pollutants, such as dyes, pharmaceuticals, pesticides, and industrial chemicals [35–37]. This process relies predominantly on the in situ generation of highly reactive oxidative species, primarily hydroxyl radicals (•OH) , which non-selectively mineralize organic contaminants into innocuous end-products like CO_2 and H_2O. Beyond organic pollutants, PEC also facilitates heavy metal reduction and immobilization, microbial pathogen inactivation, and simultaneous pollutant degradation and energy generation [38–40].

Despite these promising advances, several critical barriers remain for large-scale implementation of TiO_2-based PEC technologies, including limited visible light utilization, moderate quantum efficiencies, inadequate long-term operational stability, and challenges associated with scaling laboratory successes into commercially viable systems (Figure 2) [3,41,42]. Addressing these barriers necessitates deeper mechanistic insights into PEC processes at the materials, interfaces, and system levels, and the establishment of robust design principles for catalytic efficacy and durability. A general schematic of the photoelectrochemical (PEC) process using a TiO_2 photoanode is illustrated in Figure 1, highlighting the roles of photogenerated electrons and holes in redox reactions occurring at the photoanode and cathode.

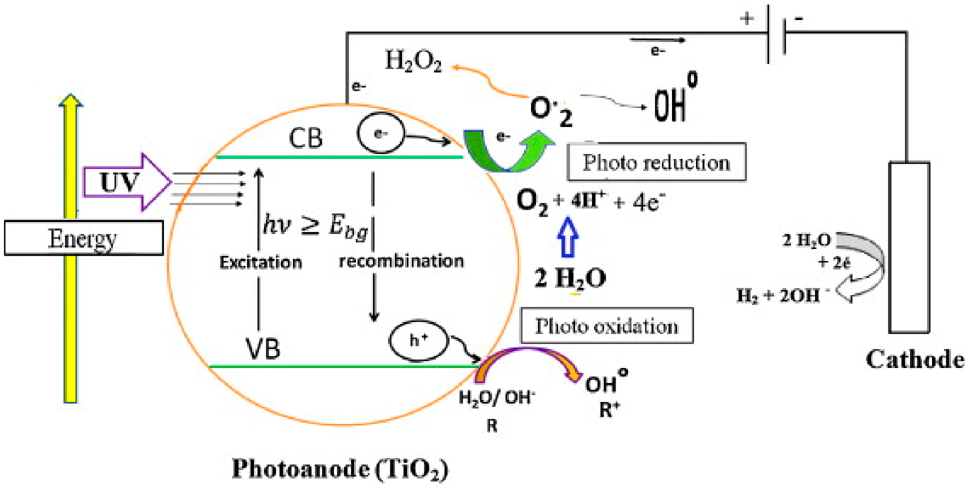

Figure 2. Schematic illustration of the PEC mechanism at a TiO_2 photoanode. Upon UV illumination, photogenerated electrons and holes drive redox reactions at the electrode surfaces, facilitating the degradation of pollutants via oxidation and reduction pathways [42]. Copyright, 2012 Elsevier.

This review critically evaluates recent advances in TiO_2-based PEC technologies, emphasizing strategies for enhanced visible light activation and improved environmental applicability. Initially, we elucidate fundamental physicochemical mechanisms underlying TiO_2 PEC, followed by an in-depth assessment of materials engineering strategies—including doping, defect modulation, heterojunction formation, and plasmonic enhancement—to expand the visible photoresponse and improve charge separation. Subsequently, we examine the environmental applications of advanced PEC systems, particularly organic contaminant degradation, water purification, and energy-related processes. Finally, we identify persistent technical challenges and explore emerging research directions, guiding the rational development of next-generation TiO_2-based PEC platforms for sustainable environmental remediation.

2. TiO_2 Photoelectrocatalysis Mechanisms

2.1. Fundamental Principles of TiO_2 Photoelectrocatalysis

Photoelectrocatalysis (PEC) represents a substantial advancement over conventional photocatalysis by coupling semiconductor-driven photophysical processes with electrochemical charge transfer reactions, effectively addressing the major limitation of rapid recombination of photogenerated electron–hole pairs (Figure 3) [43]. Upon illumination with photons possessing energies equal to or exceeding the bandgap of TiO_2 (approximately 3.2 eV for anatase, 3.0 eV for rutile) , electrons in the valence band (VB) are excited to the conduction band (CB) , generating electron–hole pairs [44,45]. The application of an external anodic bias at the TiO_2 photoanode creates an internal electric field that directs electrons towards the cathode, thus significantly reducing recombination rates [46,47]. This configuration enhances the oxidative potential of photogenerated holes (located around +2.7 V vs. NHE at neutral pH) , facilitating direct oxidation of organic pollutants and formation of reactive oxygen species (ROS) , particularly hydroxyl radicals (•OH) , leading to pollutant mineralization into CO_2 and H_2O [48,49].

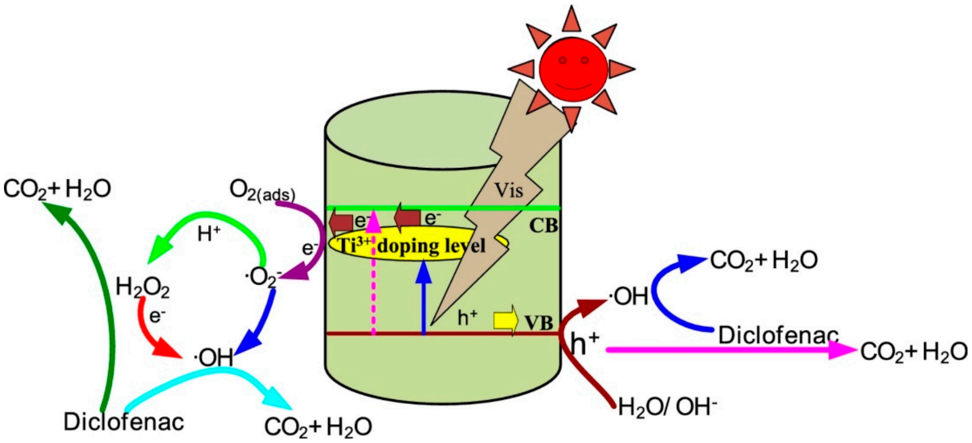

Figure 3. Principle of titanium dioxide-based photoelectrocatalysis [43]. Copyright, 2016 Elsevier.

2.2. Charge Separation and Transfer Mechanisms

The efficiency of charge separation and interfacial charge transfer in TiO_2-based PEC systems is governed by factors including the crystalline phase of TiO_2, substrate conductivity, applied external bias, and electrolyte composition [50,51]. Among the polymorphs of TiO_2—anatase, rutile, and brookite—anatase typically exhibits superior PEC performance due to its favorable conduction band potential, lower electron effective mass, and reduced charge carrier recombination [52,53]. Conductive substrates such as fluorine-doped tin oxide (FTO) , indium-doped tin oxide (ITO) , or metallic foils (e.g., titanium) enhance electron extraction and facilitate efficient charge transport [54,55]. Optimizing the semiconductor–substrate interface is essential for minimizing interfacial resistance and ensuring rapid charge transport, and this can be achieved via surface treatments, interfacial engineering, or the introduction of buffer layers.

Application of an external anodic bias leads to the formation of a space charge region (depletion layer) at the TiO_2–electrolyte interface, establishing an internal electric field that promotes directional charge carrier migration. The optimal bias voltage is closely related to the flat-band potential of TiO_2 and typically ranges between 0.5 and 1.5 V vs. Ag/AgCl reference electrode [56,57]. An inadequate bias may fail to provide sufficient driving force for charge separation, whereas an excessively high potential may initiate competing electrochemical side reactions that compromise the overall photoelectrocatalytic performance.

Real-time and *operando* spectroscopic analyses have yielded important mechanistic insights into interfacial charge dynamics during photoelectrocatalysis [58]. Ultrafast time-resolved measurements reveal that electron transfer from TiO_2 to the conductive substrate occurs on the femtosecond to picosecond scale, while hole transfer to surface-adsorbed species typically transpires over nanoseconds to microseconds [59,60]. This disparity in transfer kinetics underscores the necessity of efficient charge separation strategies to minimize recombination losses and prolong charge carrier lifetimes.

2.3. Formation of Reactive Oxygen Species

The oxidative capacity of TiO_2-based PEC systems is largely attributable to the generation of ROS, including hydroxyl radicals (•OH) , superoxide radicals ($O_2•^-$) , singlet oxygen ($^1O_2$) , and hydrogen peroxide (H_2O_2) [61,62]. Hydroxyl radicals, generated predominantly by oxidation of water or hydroxide ions at the TiO_2 surface, possess a high oxidation potential (+2.8 V vs. NHE) and effectively mineralize organic pollutants [63,64].Superoxide radicals, formed via conduction band electrons reducing molecular oxygen, contribute to pollutant degradation by producing additional ROS, such as H_2O_2 [65,66].

Hydrogen peroxide can be further activated by photogenerated electrons or UV irradiation, yielding additional hydroxyl radicals. Singlet oxygen, though less extensively studied, forms through energy transfer or secondary ROS reactions, selectively degrading certain electron-rich pollutants [67].

2.4. Reaction Kinetics and Degradation Pathways

Organic pollutant degradation kinetics in TiO_2 PEC generally follow the Langmuir–Hinshelwood (L–H) model, accounting for pollutant adsorption and subsequent oxidative surface reactions [68,69]. At dilute pollutant concentrations, kinetics simplify to pseudo-first-order behavior. Oxidative degradation initiates with hydroxyl radical attacks on electron-rich functional groups, forming hydroxylated intermediates, which subsequently undergo ring-opening and further oxidation to short-chain organic acids, ultimately mineralizing into CO_2 and H_2O. An illustrative example is the degradation of bisphenol A, involving sequential hydroxylation, oxidative ring cleavage, and mineralization, demonstrating the effectiveness of PEC for detoxifying complex organic pollutants [70]. As shown in Figure 4 [71], under solar irradiation, photoexcited electrons and holes are separated and participate in surface reactions. Metal doping enhances charge separation, while the generated hydroxyl radicals attack pollutant molecules, ultimately leading to complete mineralization into CO_2 and H_2O.

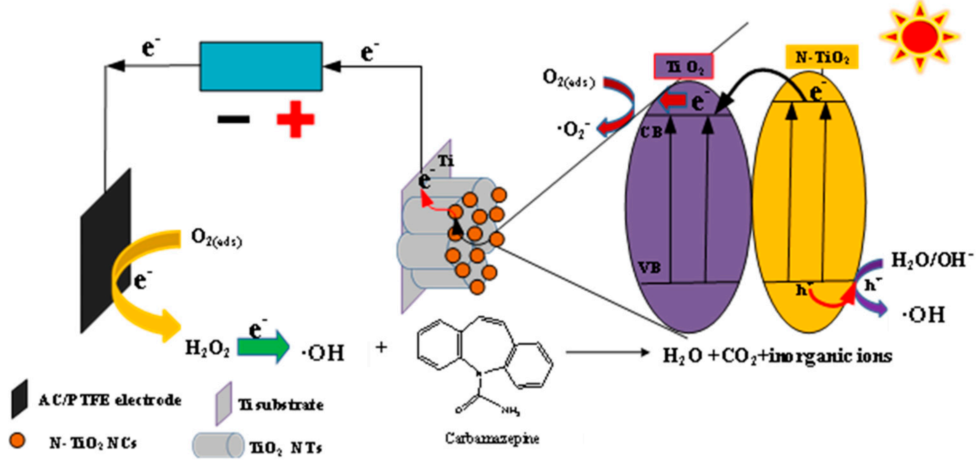

Figure 4. Schematic illustration of the PEC mechanism for organic pollutant degradation. Metal-doped TiO_2 (M-TiO_2) enhances charge separation, facilitates •OH radical formation, and promotes the stepwise oxidation of organic molecules under visible light irradiation [71]. Copyright, 2024, MDPI.

2.5. Factors Affecting TiO_2 Photoelectrocatalytic Efficiency

The overall performance of TiO_2-based PEC systems is influenced by intrinsic material properties and operational parameters, including crystalline phase composition, film thickness, external bias, illumination conditions, electrolyte pH, and inorganic ions. Anatase–rutile composites, notably commercial P25 (approximately 80% anatase and 20% rutile) , typically exhibit superior PEC performance due to enhanced interfacial charge separation [72]. Optimal TiO_2 film thickness balances

doi:10.20944/preprints202504.1178.v1

photon absorption efficiency with minimal recombination [73]. Applied external bias significantly influences charge carrier separation and recombination, with excessive potentials potentially triggering unwanted side reactions [74]. Light intensity and wavelength dictate electron–hole generation rates; unmodified TiO_2 requires ultraviolet excitation unless engineered for visible-light activation [75]. Electrolyte pH modulates surface charge, pollutant adsorption, and ROS generation; acidic conditions favor pollutant adsorption, whereas alkaline conditions enhance hydroxyl radical formation. Inorganic ions, such as phosphate and carbonate, may act as ROS scavengers, whereas chloride ions can form reactive chlorine species, potentially assisting pollutant degradation [76]. A comprehensive understanding of these parameters is essential to optimize TiO_2 PEC systems, enhancing their applicability for practical environmental remediation.

3. TiO_2 Modification Strategies for Enhanced Visible Light Response

Although TiO_2 exhibits numerous desirable properties—such as high intrinsic photocatalytic activity, excellent chemical stability, non-toxicity, and cost-effectiveness—its practical application in photoelectrocatalysis is largely limited by two intrinsic limitations: (1) a wide bandgap (3.0–3.2 eV) , which restricts its photoactivity to the ultraviolet (UV) region, accounting for only ~5% of the solar spectrum, and (2) the rapid recombination of photogenerated electron–hole pairs, which significantly reduces quantum efficiency [26]. To overcome these limitations and extend its photoresponse into the visible region, a variety of modification strategies have been proposed. This section provides a comprehensive overview of these approaches, including elemental doping, defect engineering, heterojunction construction, and the exploitation of surface plasmon resonance (SPR) effects.

3.1. Doping Strategies

Doping refers to the intentional introduction of foreign atoms into the TiO_2 lattice to alter its electronic band structure and enhance its light-harvesting and charge-transport characteristics. Based on the dopant species, doping strategies are generally categorized into metal and non-metal doping.

3.1.1. Metal Doping

Metal doping involves the incorporation of metal ions into the TiO_2 crystal lattice, either substitutionally (replacing Ti^{4+} ions) or interstitially. Metal dopants can introduce mid-gap energy levels, thereby enabling the absorption of visible light and facilitating interband electronic transitions [77]. Furthermore, certain metal ions act as electron or hole traps, suppressing recombination and improving charge separation efficiency. These effects are further supported by both theoretical and experimental data, as shown in Figure 5 [78]. Density of states (DOS) calculations and EELS spectra indicate that doping with B and N introduces mid-gap states, narrows the bandgap, and modifies the electronic structure of TiO_2. The schematic diagram further illustrates the band alignment and energy transitions resulting from core-shell doping structures.

Among transition metals, cerium (Ce) doping has shown considerable promise. For example, Ce-doped TiO_2 photoanodes have demonstrated enhanced performance in the photoelectrocatalytic reduction of CO_2 to C_2 products under visible light [79]. The incorporation of Ce^{4+} not only narrows the bandgap via intermediate states but also functions as an electron trap, facilitating charge separation. A Faradaic efficiency of up to 68% for ethanol and acetate production was achieved, highlighting the dual role of Ce in light absorption and charge management.

Similarly, cobalt (Co) doping in ZnO lattices has been explored to extend light absorption into the visible region. Substitution of Zn^{2+} with Co^{2+} introduces intra-bandgap states, enhancing visible light harvesting and improving photocatalytic performance. Compared to Ag–ZnO photoanodes, $Zn_{1-x}Co_xO$ systems exhibited superior photoelectrocatalytic activity owing to more effective charge separation and enhanced light absorption [80].

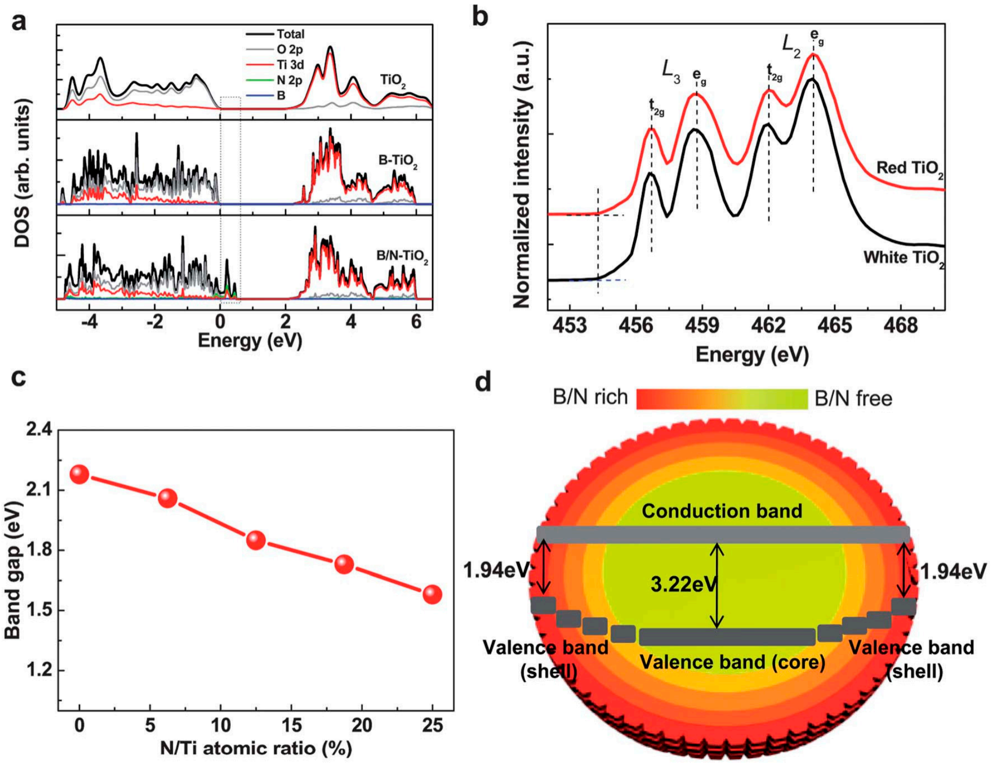

Figure 5. Electronic structure characterization of modified TiO_2: (a) Density of states (DOS) for pristine anatase TiO_2, interstitial $[BO_4]$-doped (B-TiO_2) , and $[BO_{4-x}N_x]$ co-doped (B/N-TiO_2) systems; (b) Ti L-edge XANES spectra comparing white and red TiO_2; (c) Bandgap tuning via N/Ti atomic ratio variation in B-doped anatase; (d) Schematic band structure of gradient-bandgap red TiO_2 [78]. Copyright, Royal Society of Chemistry Group.

Noble metal doping—particularly with Pd, Pt, and Au—provides additional benefits via multiple mechanisms. These metals can serve as electron sinks, promote interfacial charge transfer through Schottky junction formation, and induce localized surface plasmon resonance (LSPR) , which enhances visible light absorption. For instance, Pd-decorated ZnO photoanodes have demonstrated improved degradation of paracetamol under visible light, attributed to LSPR-induced light absorption and efficient electron–hole separation facilitated by Schottky barriers at the Pd–ZnO interface [81].

Nonetheless, excessive doping concentrations may lead to the formation of recombination centers or disrupt lattice periodicity, thereby reducing photocatalytic efficiency. Therefore, careful optimization of dopant type and concentration is essential to balance light absorption and carrier transport.

3.1.2. Non-Metal Doping

Non-metal doping entails the incorporation of light elements—such as nitrogen (N) , carbon (C) , sulfur (S) , boron (B) , and fluorine (F) —into the TiO_2 lattice, often substituting for lattice oxygen. These dopants modulate the valence band structure by introducing impurity states or hybridizing their *p* orbitals with O 2p states, thereby narrowing the bandgap and enabling visible light activation [29].

Nitrogen doping is among the most extensively investigated non-metal doping strategies. N-doped TiO_2 exhibits a notable red shift in its absorption spectrum, attributable to the introduction of N 2p states above the valence band maximum, which reduces the effective bandgap. For instance, N-doped TiO_2 photoanodes have shown enhanced degradation of methylene blue under visible light, outperforming pristine TiO_2, which remains inactive under the same conditions [82].

Sulfur doping has also demonstrated efficacy in extending the photoresponse into the visible region. The incorporation of S 3p orbitals into the TiO_2 valence band reduces the bandgap and

doi:10.20944/preprints202504.1178.v1

promotes light absorption. For example, S-doped Mn–TiO_2 photoanodes exhibited enhanced degradation of ribavirin under visible light, owing to the synergistic effects of S-induced bandgap narrowing and Mn-facilitated charge separation [83].

Carbon doping, another widely explored strategy, can occur via substitutional or interstitial incorporation, or through surface modification with carbonaceous species such as carbon quantum dots (CQDs) . C-doped TiO_2 exhibits red-shifted absorption spectra, improved carrier separation, and enhanced photoelectrocatalytic activity. CQD-modified TiO_2, in particular, has demonstrated superior performance due to the dual role of CQDs in expanding light absorption and facilitating electron transfer via their excellent electron-accepting capabilities [84].

Co-doping with multiple non-metallic elements has emerged as a promising approach for synergistic bandgap modulation and charge separation enhancement. For example, N,S-co-doped TiO_2 has been shown to outperform singly doped counterparts in both light absorption and photoelectrocatalytic efficiency under visible light, owing to improved orbital hybridization and extended carrier lifetimes [85].

3.2. Defect Engineering

Defect engineering entails the deliberate manipulation of crystal imperfections within the TiO_2 lattice to tailor its electronic structure, optical absorption characteristics, and photoelectrocatalytic performance. These defects can be broadly categorized into intrinsic types—such as oxygen vacancies and titanium interstitials—and extrinsic types, including dopant-induced lattice distortions and surface imperfections. Among them, oxygen vacancies have garnered the most attention due to their pronounced impact on visible light absorption and charge carrier dynamics.

Oxygen vacancies act as shallow donor states, introducing mid-gap energy levels that extend the optical absorption edge of TiO_2 into the visible spectrum [30]. In addition to enhancing light absorption, these vacancies increase carrier concentration and conductivity by acting as electron donors. Moreover, they serve as electron trapping sites, thereby facilitating charge separation and suppressing bulk recombination. Various methodologies have been employed to generate oxygen vacancies in TiO_2, including thermal annealing in reducing atmospheres, hydrogenation, plasma exposure, and chemical reduction processes.

Surface defect engineering via acid treatment has also been shown to significantly improve the PEC performance of TiO_2. For example, hydrofluoric acid (HF) treatment of TiO_2 nanotubes resulted in increased concentrations of surface oxygen vacancies, which enhanced visible light absorption and improved interfacial charge separation [86]. The treated nanotubes exhibited a 2.5-fold increase in the degradation rate of methylene blue compared to their pristine counterparts—an improvement attributed to the synergistic effects of light absorption and defect-induced charge management.

Furthermore, three-dimensional titanium substrates supporting TiO_2 nanotube arrays have been reported to induce a higher density of interface-specific defects, particularly at the nanotube–substrate junction. This architectural configuration promotes superior charge transport and spatial separation of photogenerated carriers, yielding enhanced PEC activity relative to conventional two-dimensional arrays [87].

Nevertheless, it is essential to note that an excessive concentration of defects may act as deep-level recombination centers, ultimately diminishing photocatalytic performance. Thus, fine-tuning the defect density and distribution is critical for maximizing PEC efficiency.

3.3. Heterojunction Construction

Constructing heterojunctions by coupling TiO_2 with other semiconductors offers an effective strategy to enhance light absorption, suppress charge recombination, and promote interfacial charge transfer. Depending on the relative band alignment of the constituent semiconductors, heterojunctions are commonly classified into three types: Type I (straddling gap) , Type II (staggered gap) , and Type III (broken gap) . Among these, Type II heterojunctions are most widely employed in PEC systems due to their efficient charge separation behavior.

3.3.1. TiO_2-Based p–n Heterojunctions

p–n heterojunctions are formed by interfacing n-type TiO_2 with p-type semiconductors, such as Cu_2O, CuO, NiO, and BiOX (X = Cl, Br, I) . The built-in electric field at the junction interface facilitates the spatial separation of photogenerated charge carriers—electrons migrate toward the n-type region, while holes are directed toward the p-type domain—thereby suppressing recombination and enhancing PEC activity [88].

However, conventional p–n junctions formed by TiO_2 and simple metal oxides often exhibit limited carrier mobility and recombination suppression. Hence, more sophisticated designs are needed. A notable advancement is the piezoelectric-enhanced n-TiO_2/$BaTiO_3$/p-TiO_2 heterostructure, which exhibited significantly improved PEC performance under visible light (Figure 6) [89]. Here, the introduction of $BaTiO_3$, a piezoelectric material, enabled an additional electric field under mechanical deformation, which further promoted charge separation beyond the built-in field of the p–n junction. This system achieved a 3.2-fold improvement in methylene blue degradation efficiency relative to pristine TiO_2. This rationally designed p–n heterojunction with a ferroelectric interlayer not only improves charge transport across interfaces but also modulates the internal electric field, thereby boosting the overall PEC performance.

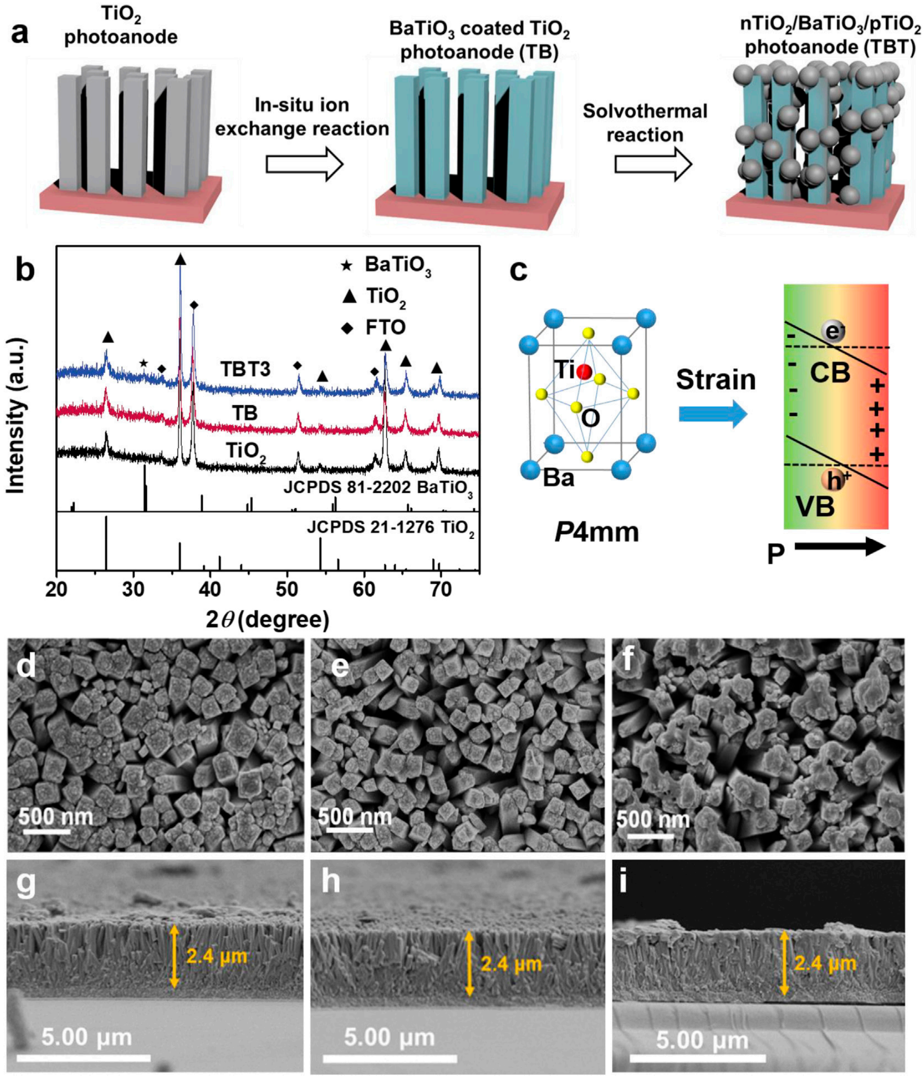

Figure 6. (a) Schematic illustration of the fabrication process of the TBT (nTiO_2/$BaTiO_3$/pTiO_2) photoanode via in situ ion exchange and solvothermal treatment. (b) XRD patterns confirming the presence of $BaTiO_3$ and TiO_2 phases. (c) Schematic representation of strain-induced band structure modulation introduced by Ba^{2+} incorporation. (d–f) Top-view SEM images, and (g–i) cross-sectional

SEM images showing uniform multilayer morphology and film thickness (~2.4 μm) [89]. Copyright, 2024 Elsevier.

Similarly, a ferroelectric-enhanced $BiVO_4/BiFeO_3$ p–n heterojunction demonstrated superior performance for the photoelectrocatalytic degradation of tetracycline [90]. The spontaneous polarization of $BiFeO_3$ contributed an internal electric field that further assisted charge dissociation at the junction, highlighting the benefit of integrating ferroelectric components into PEC architectures.

3.3.2. TiO_2-Based Z-Scheme Heterojunctions

Z-scheme heterojunctions are bioinspired architectures that emulate the natural photosynthetic electron transfer chain. They couple two semiconductors via a solid-state electron mediator or direct interface contact, allowing photogenerated electrons from one semiconductor to recombine with holes from the other. This configuration retains the strong redox potential of each component and promotes spatial charge separation [91].

Another sophisticated example is the multi-interface polarization-engineered 1T–2H MoS_2/TiO_2 Z-scheme system (Figure 7) [92]. The internal phase boundaries between metallic 1T and semiconducting 2H MoS_2 phases created localized electric fields, which, in conjunction with the TiO_2 interface, reinforced charge separation. The system exhibited superior PEC performance under visible light, affirming the advantages of engineered interfacial polarization.

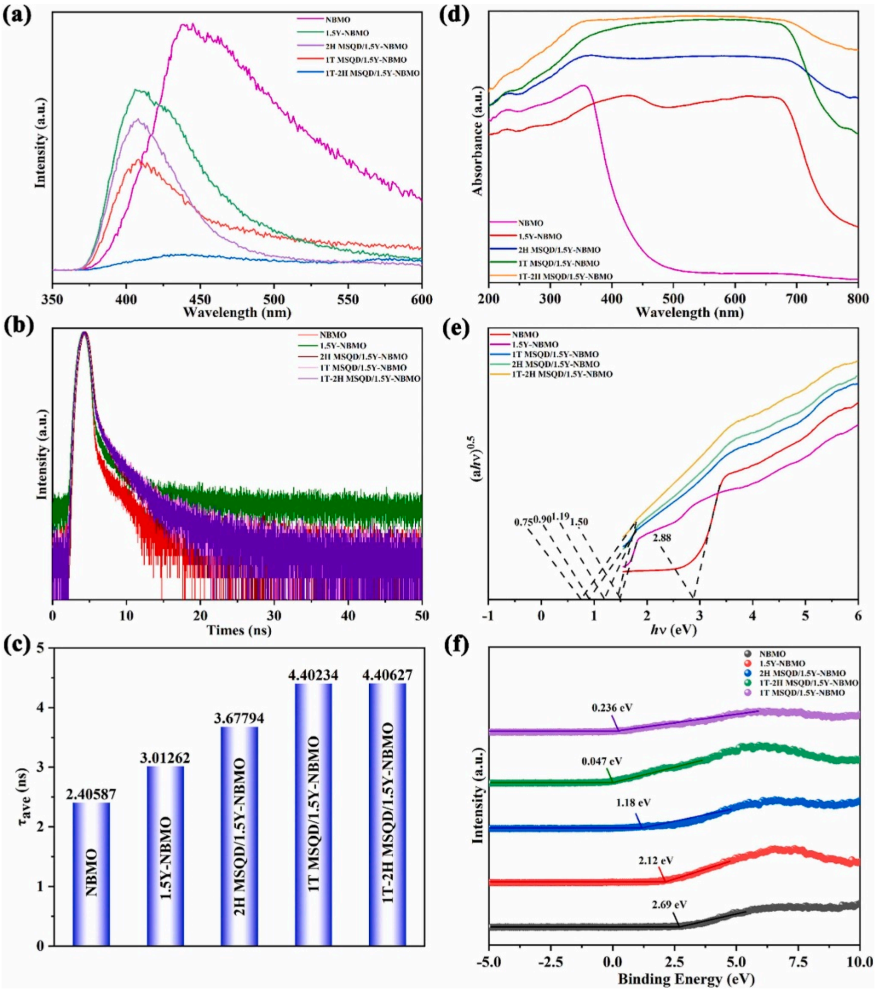

Figure 7. (a) Steady-state PL spectra of different photoanodes. (b) Time-resolved PL decay curves. (c) Flat-band potential values derived from Mott–Schottky plots. (d) UV–vis absorption spectra. (e) Tauc plots for estimating bandgaps. (f) XPS valence band spectra for determining the valence band maximum and estimating band alignment [92]. Copyright, 2023 Elsevier.

doi:10.20944/preprints202504.1178.v1

3.3.3. TiO_2-Based Carbon Material Heterojunctions

The integration of TiO_2 with conductive carbonaceous materials—such as graphene, carbon nanotubes (CNTs) , and CQDs—has emerged as a promising approach to enhance PEC performance by improving charge carrier dynamics and light absorption [93]. Carbon materials act as electron acceptors, facilitating directional charge transfer and mitigating recombination. Additionally, their high conductivity and surface area contribute to improved photon utilization and electrolyte interaction.

Two-dimensional graphitic materials, particularly graphene and its derivatives, have been widely employed to construct TiO_2-based heterojunctions [94]. The exceptional electrical conductivity, large specific surface area, and mechanical flexibility of graphene promote efficient electron transport and extended light harvesting. Graphene–TiO_2 composites have demonstrated enhanced degradation of organic dyes under visible light due to improved charge carrier separation and sensitization effects.

Mechanistic studies on graphene–TiO_2 photoanodes revealed that graphene serves as an efficient electron sink, accepting electrons from the TiO_2 conduction band and preventing their recombination with photogenerated holes [95].

More advanced architectures, such as hierarchical TiO_2 nanowire arrays grown on graphite fibers, have been shown to further enhance interfacial contact and charge separation [96]. The graphite fiber substrate acts as an efficient electron collector, facilitating rapid carrier extraction and reducing recombination, resulting in significantly improved pollutant degradation.

3.4. Surface Plasmon Resonance Effects

Surface plasmon resonance (SPR) refers to the coherent oscillation of conduction band electrons at the interface between a metal nanoparticle and a dielectric medium when irradiated with light at a resonant frequency . SPR-active nanostructures can significantly enhance the photoelectrocatalytic (PEC) performance of TiO_2 via several mechanisms, including: (i) local electromagnetic field enhancement, (ii) hot electron injection into the semiconductor, and (iii) broadening of the light absorption spectrum into the visible region.

3.4.1. Noble Metal Plasmonics

Noble metals such as Au, Ag, and Pt exhibit strong SPR phenomena in the visible spectrum, making them highly effective in extending the photoresponse of TiO_2. Upon photoexcitation, the SPR-induced hot electrons in these metals can be transferred to the conduction band of TiO_2, thereby initiating redox reactions under visible light.

For instance, Ag-decorated V_2O_5–TiO_2 nanocomposites have exhibited remarkable PEC activity for organic pollutant degradation under visible light [97]. The localized SPR of Ag nanoparticles not only enhanced photon absorption but also facilitated hot electron injection into the TiO_2 conduction band. As a result, the plasmonic system demonstrated a 4.1-fold increase in methylene blue degradation compared to pristine TiO_2.

Similarly, Ag–ZnO photoanodes have shown enhanced PEC efficiency due to SPR-assisted charge separation [80]. In this system, Ag nanoparticles served as both light-harvesting centers and electron donors, thereby improving visible light utilization and carrier mobility.

3.4.2. Non-Noble Metal Plasmonics

To mitigate the cost and scarcity of noble metals, significant efforts have been directed toward exploring non-noble metal plasmonic materials—such as Cu, Al, and transition metal nitrides—that exhibit SPR-like behavior in the visible and near-infrared regions [98].

Copper-based plasmonic TiO_2 photocatalysts have shown promising results for the degradation of organic pollutants under solar irradiation [120]. Cu nanoparticles deposited on TiO_2 surfaces introduced visible light activity via SPR, while simultaneously improving charge separation through hot electron transfer mechanisms. The Cu–TiO_2 system outperformed pristine TiO_2 under comparable irradiation conditions, demonstrating its potential as a cost-effective plasmonic alternative.

3.4.3. Synergistic Plasmonic–Semiconductor Hybrid Systems

Integrating SPR-active materials with other modification strategies—such as elemental doping and heterojunction engineering—can yield synergistic effects that substantially enhance PEC performance.

For example, Ag-decorated N-doped TiO_2 systems have demonstrated superior PEC activity under visible light compared to their individually modified counterparts [99]. The synergistic effect arises from the combination of SPR-induced hot electron generation (from Ag) and bandgap narrowing (from nitrogen doping) , both of which contribute to improved light absorption and charge transport.

Similarly, Ag nanoparticle-decorated TiO_2–graphene heterojunctions have shown notable performance enhancements due to dual mechanisms: plasmonic excitation and interfacial charge transfer [31]. The interfacial synergy between the TiO_2 semiconductor, graphene electron conductor, and Ag plasmonic sensitizer resulted in significantly improved pollutant degradation under visible light.

3.5. Other Modification Strategies

Beyond the widely investigated strategies, several emerging modification approaches have been developed to further expand the visible light activity of TiO_2-based PEC systems.

3.5.1. Conductive Polymer Functionalization

Conductive polymers—including polyaniline (PANI) , polypyrrole (PPy) , and poly (3,4-ethylenedioxythiophene) (PEDOT) —offer tunable optoelectronic properties and have been successfully incorporated into TiO_2-based materials to extend light absorption and improve interfacial charge transport.

For instance, electrically conductive TiO_2–PANI–PVDF composite membranes have shown significantly improved PEC degradation of organic pollutants under visible light (Figure 8) [100]. The incorporation of PANI enhanced light absorption and facilitated electron transport, owing to its π-conjugated structure and favorable energy alignment with TiO_2. Similarly, PEDOT-modified PVDF membranes embedded with TiO_2 nanoparticles exhibited a 2.8-fold improvement in methylene blue degradation efficiency, attributed to improved conductivity and enhanced charge separation.

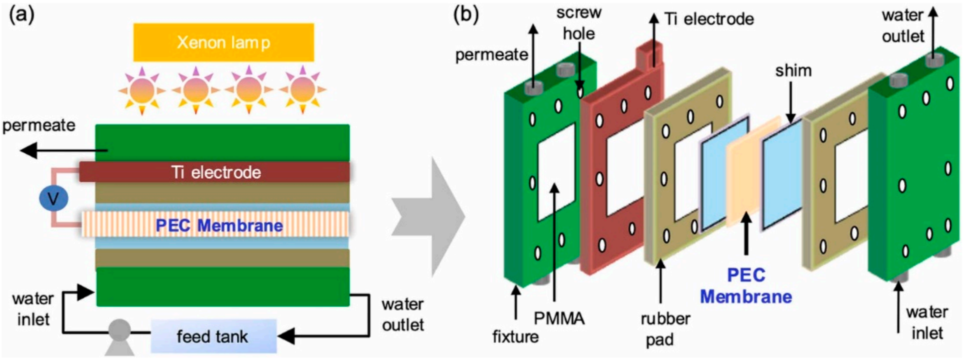

Figure 8. (a) Schematic diagram of the membrane-integrated photoelectrochemical (PEC) reactor under light illumination. (b) Exploded view of the assembled PEC system showing the structural components, including Ti electrodes, PEC membrane, sealing gaskets, and flow channels [100]. Copyright, 2022 Elsevier.

3.5.2. Organic Dye Sensitization

Dye sensitization is a classical strategy adapted from dye-sensitized solar cells (DSSCs) , wherein organic dyes adsorbed onto TiO_2 surfaces absorb visible light and inject excited electrons into the TiO_2 conduction band. This expands the spectral response of TiO_2 into the visible region, enabling PEC reactions under solar irradiation.

Various dyes—including ruthenium complexes, porphyrins, and natural pigments—have been employed to sensitize TiO_2. N719-sensitized TiO_2 photoanodes, for example, exhibited marked improvements in PEC degradation of methylene blue under visible light, in contrast to the negligible activity of unmodified TiO_2 [36].

3.5.3. Coupling with Energy Harvesting Systems

The integration of TiO_2 PEC systems with self-powered energy harvesting devices—such as triboelectric and piezoelectric nanogenerators—has emerged as a cutting-edge approach for enhancing performance and energy autonomy.

To achieve a fully self-powered photoelectrochemical (PEC) system, we integrated a rotational electromagnetic energy harvester with the photoanode module. This device converts mechanical energy into electrical energy in real time, enabling bias-free PEC reactions under ambient conditions. A representative system combining a triboelectric–electromagnetic nanogenerator with a TiO_2-based Type II heterojunction was demonstrated for water treatment applications (Figure 9) [101]. Mechanical energy harvested from water flow was converted into electrical energy, which provided an external bias to drive charge separation in the PEC system. The self-powered configuration showed significantly enhanced degradation of pollutants, even under low light intensity conditions, underscoring the potential of hybrid energy–catalysis platforms.

Collectively, these diverse modification strategies offer promising routes for overcoming the intrinsic limitations of TiO_2, particularly its wide bandgap and rapid charge recombination. Through synergistic integration of multiple enhancement approaches—such as doping, heterojunction engineering, plasmonic sensitization, and hybrid coupling with functional materials—TiO_2-based PEC systems can achieve substantially improved performance under visible light irradiation. Continued advancements in material design, interface engineering, and system integration will be critical to translating laboratory-scale innovations into scalable solutions for solar-driven environmental remediation.

Preprints.org (www.preprints.org) | NOT PEER-REVIEWED | Posted: 15 April 2025 doi:10.20944/preprints202504.1178.v1

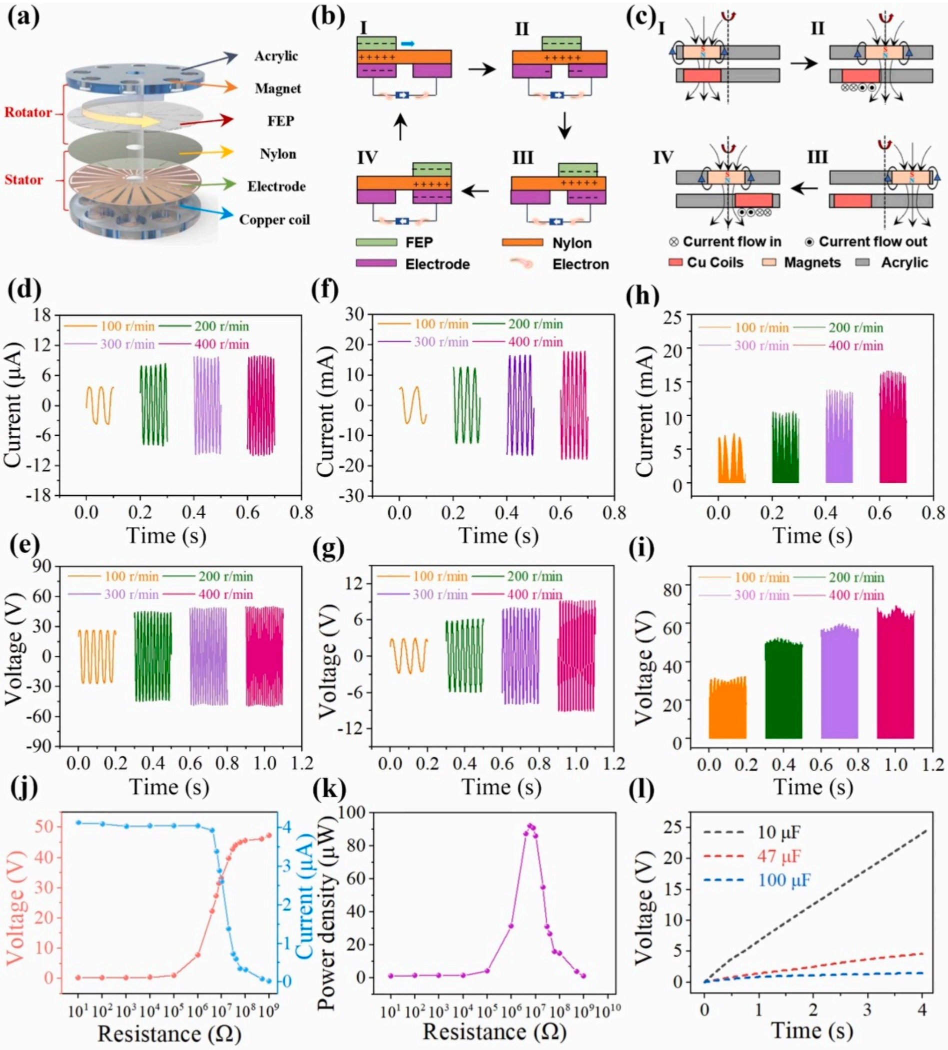

Figure 9. (a) Structural layout of the electromagnetic nanogenerator composed of multilayer components including FEP film, nylon electrode, and copper coil. (b, c) Working mechanism illustrations showing current generation during rotation. (d–i) Output current and voltage waveforms at different rotation speeds. (j) Load-dependent voltage and current output. (k) Power output as a function of resistance. (l) Capacitor charging curves under generator operation [101]. Copyright, 2025 Elsevier.

4. Environmental Applications of TiO_2-Based Photoelectrocatalysis

TiO_2-based photoelectrocatalysis (PEC) has garnered increasing attention as a promising solution to various environmental issues, particularly in the context of advanced water and wastewater treatment. By combining photocatalytic oxidation with electrochemical bias-induced charge separation, TiO_2-based systems exhibit superior pollutant degradation efficiency and enhanced operational robustness. The integration of advanced material modifications—such as doping, heterojunction construction, and plasmonic enhancement—further broadens their applicability. This section highlights key environmental applications of TiO_2-based PEC, with an emphasis on the degradation of organic contaminants, disinfection, and coupled energy conversion processes.

4.1. Organic Pollutant Degradation

The removal of persistent organic pollutants (POPs) constitutes one of the most widely explored applications of TiO_2-based PEC. Compared with conventional treatment technologies, PEC offers several distinct advantages: high redox potential, non-selective reactivity, and the capability for complete mineralization of contaminants into CO_2 and H_2O.

4.1.1. Pharmaceutical Compounds

Pharmaceuticals, including antibiotics, analgesics, and endocrine disruptors, are frequently detected in aquatic systems due to widespread consumption, partial human metabolism, and limited removal efficiency in conventional wastewater treatment plants. TiO_2-based PEC systems have demonstrated remarkable potential in degrading such micropollutants under controlled conditions.

For instance, paracetamol (acetaminophen) , a widely consumed analgesic, has been efficiently degraded using TiO_2 photoanodes [102]. Comparative studies revealed that PEC achieved a degradation efficiency of 95%, outperforming both photocatalysis (78%) and electrochemical oxidation (65%) under identical conditions. This enhanced performance was attributed to efficient electron–hole separation under external bias, which promoted both direct oxidation by holes and indirect oxidation via hydroxyl radical formation.

Levofloxacin, a fluoroquinolone antibiotic, was also efficiently removed through PEC with TiO_2 photoanodes, achieving >92% degradation within 60 minutes under UV irradiation and optimized bias (1.0 V, pH 7) (Figure 10) [103]. The degradation kinetics followed a pseudo-first-order model, driven by hydroxyl radical attack on the aromatic ring system.

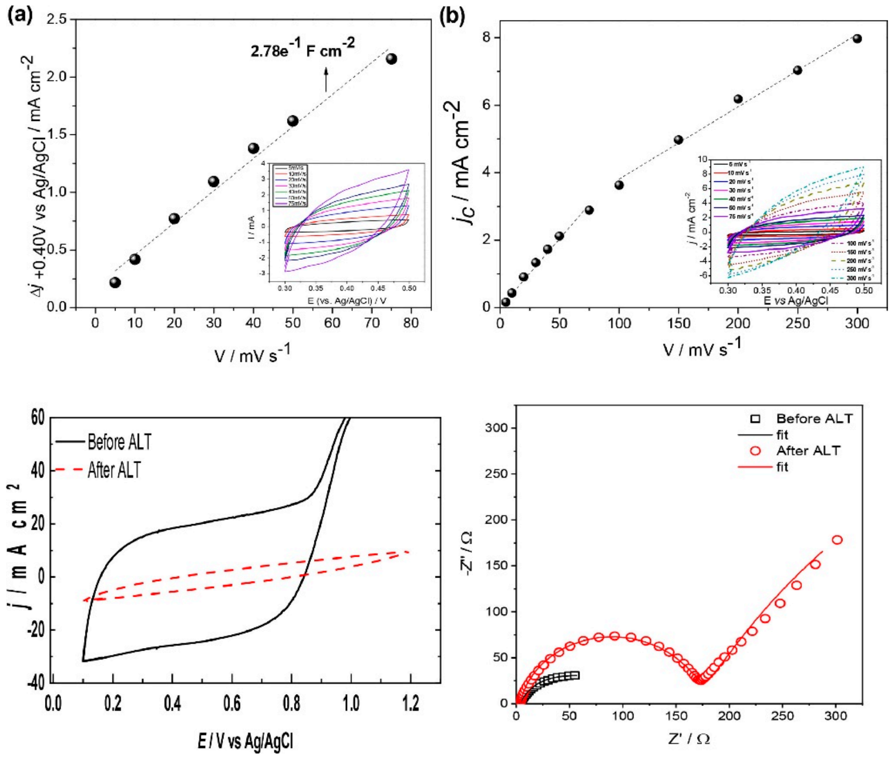

Figure 10. Relationship between capacitive current density (average) at +0.40 V and different scan rates applied (5 – 75 mV s^{-1}) for the ECSA analysis [103]. Copyright, 2024 Elsevier.

4.1.2. Dyes and Pigments

Synthetic dyes—such as azo, anthraquinone, and triphenylmethane compounds—are prevalent in industrial effluents and are known for their high stability and toxicity. PEC treatment offers an effective approach for the breakdown of these chromophores.

A study on the degradation of methylene blue (cationic) and congo red (anionic) revealed that electrostatic interactions with the TiO_2 surface play a critical role [104]. At near-neutral pH, the negatively charged TiO_2 surface facilitated the adsorption of cationic species, resulting in higher removal efficiency for methylene blue.

4.1.3. Pesticides and Herbicides

The widespread use of agrochemicals has led to frequent contamination of natural water bodies with toxic pesticides and herbicides. TiO_2-based PEC systems have shown efficacy in degrading structurally diverse compounds such as atrazine, 2,4-D, and chlorpyrifos.

In the case of atrazine, TiO_2 nanotube arrays achieved 98% degradation within 120 minutes under acidic conditions (pH 3) and a 2.0 V bias [105]. The process followed pseudo-first-order kinetics and was governed primarily by •OH-mediated oxidative attack on the triazine ring.

For 2,4-dichlorophenoxyacetic acid (2,4-D) , PEC treatment using TiO_2 nanotubes under a 1.5 V bias significantly enhanced removal efficiency compared to photocatalysis alone [106]. Identified intermediates indicated successive dechlorination and oxidation steps, again emphasizing the central role of hydroxyl radicals in pollutant breakdown.

4.1.4. Industrial Chemicals

Industrial effluents typically contain complex mixtures of phenols, halogenated organics, and other recalcitrant aromatic compounds. The non-selective oxidative capability of TiO_2-based PEC systems makes them ideal for treating such wastewater.

For example, the mineralization of phenol was significantly improved by coupling PEC with ozonation, achieving 95% total organic carbon (TOC) removal, compared to 78% and 65% for standalone PEC and ozonation, respectively [107]. The synergy was attributed to the generation of additional •OH radicals via ozone–electron interactions.

In another study, reduced graphene oxide (rGO) -modified TiO_2 photoanodes facilitated enhanced degradation of p-chloronitrobenzene, a persistent industrial pollutant [108]. The incorporation of rGO extended visible light absorption and improved electron mobility, resulting in 92% degradation within 60 minutes under visible light—compared to only 45% with unmodified TiO_2.

These findings collectively demonstrate the versatility of TiO_2-based PEC systems in addressing a wide range of organic contaminants. Through careful control of operational parameters (e.g., pH, bias potential) and material modifications (e.g., nanotube structures, carbon-based composites) , high-efficiency degradation can be achieved even for structurally complex and recalcitrant pollutants.

4.2. Water Treatment and Disinfection

In addition to the degradation of organic pollutants, TiO_2-based photoelectrocatalysis (PEC) has exhibited considerable potential in broader water treatment applications, including heavy metal removal, microbial inactivation, and the remediation of industrial wastewaters. The synergistic combination of photocatalysis and electrochemical reduction/oxidation processes enables spatially resolved redox reactions, facilitating the concurrent removal of diverse contaminants.

4.2.1. Heavy Metal Removal

Heavy metals such as chromium, lead, mercury, and cadmium are of environmental concern due to their high toxicity, persistence, and bio accumulative nature. TiO_2-based PEC enables their removal primarily through reductive transformation at the photocathode.

For example, efficient removal of Cr (VI) from tannery wastewater was achieved using TiO_2 photoelectrodes, with a reported reduction efficiency of 99% within 60 minutes under acidic conditions (pH 3, 1.0 V bias, UV light) [109]. The mechanism involved photogenerated electron-induced reduction of Cr (VI) to Cr (III) , followed by precipitation as $Cr(OH)_3$ at elevated pH.

Interestingly, Cr (VI) itself can function as an electron scavenger in PEC systems, enhancing charge separation by capturing photogenerated electrons and thereby promoting oxidative degradation of co-existing organic pollutants [110]. This dual role of Cr (VI) contributes to a synergistic removal effect in complex wastewater matrices.

Simultaneous removal of methylene blue (95%) and Cr (VI) (98%) under solar irradiation within 90 minutes has also been demonstrated [111]. This dual functionality underscores the advantage of PEC systems in spatially decoupling oxidation (at the photoanode) and reduction (at the cathode) processes.

4.2.2. Disinfection and Microbial Inactivation

Microbial contamination, including pathogenic bacteria, viruses, and protozoa, poses a serious public health risk. PEC disinfection provides an advanced alternative to traditional chlorination, offering pathogen inactivation without harmful byproducts.

Capacitive TiO_2 photoanodes operated under external bias have shown significantly improved bactericidal performance, attributed to enhanced charge separation and the generation of reactive oxygen species (ROS) , including hydroxyl radicals and singlet oxygen [112]. These ROS induce oxidative damage to microbial membranes and intracellular components, leading to cell lysis.

4.2.3. Treatment of Complex Wastewaters

Industrial wastewaters often exhibit high chemical oxygen demand (COD) , contain diverse organic and inorganic pollutants, and are challenging to treat via conventional means. TiO_2-based PEC, due to its strong oxidizing power and non-selectivity, is well-suited for these applications.

For instance, a COD removal efficiency of 85% was achieved from gas field produced water within 120 minutes using TiO_2 nanotube array photoanodes under 2.0 V bias and UV irradiation [113]. The efficacy was primarily driven by in situ generation of ROS that oxidized a broad spectrum of organic constituents.

4.3. Energy Conversion Applications

In addition to environmental remediation, TiO_2-based PEC systems offer opportunities for solar-driven energy conversion, particularly in CO_2 reduction to value-added fuels and hydrogen evolution through water splitting. These applications align with the dual goals of environmental sustainability and renewable energy production.

4.3.1. CO_2 Reduction

The photoelectrocatalytic reduction of CO_2 to fuels or commodity chemicals addresses both carbon neutrality and energy security. TiO_2 photoanodes, when appropriately modified, have shown promising activity for CO_2 conversion under visible light.

A Cu-modified TiO_2 system achieved a Faradaic efficiency of 85% for formate production under visible light, attributed to efficient charge separation and Cu-mediated CO_2 reduction catalysis [114]. The presence of Cu facilitated multi-electron transfer processes and stabilized CO_2 intermediates on the electrode surface.

4.3.2. Water Splitting for Hydrogen Generation

PEC water splitting for hydrogen production is an attractive pathway for sustainable energy conversion. TiO_2-based systems utilize photogenerated holes for water oxidation at the photoanode and electrons for proton reduction at the cathode. TiO_2 has served as the cornerstone of PEC water splitting research since the seminal Honda–Fujishima discovery in 1972. Despite its outstanding photostability, its wide bandgap limits solar spectrum utilization, necessitating intensive modification efforts. Recent advancements, including cocatalyst loading and heterojunction engineering, have notably improved its hydrogen evolution efficiency under visible light. (Figure 10) [115].

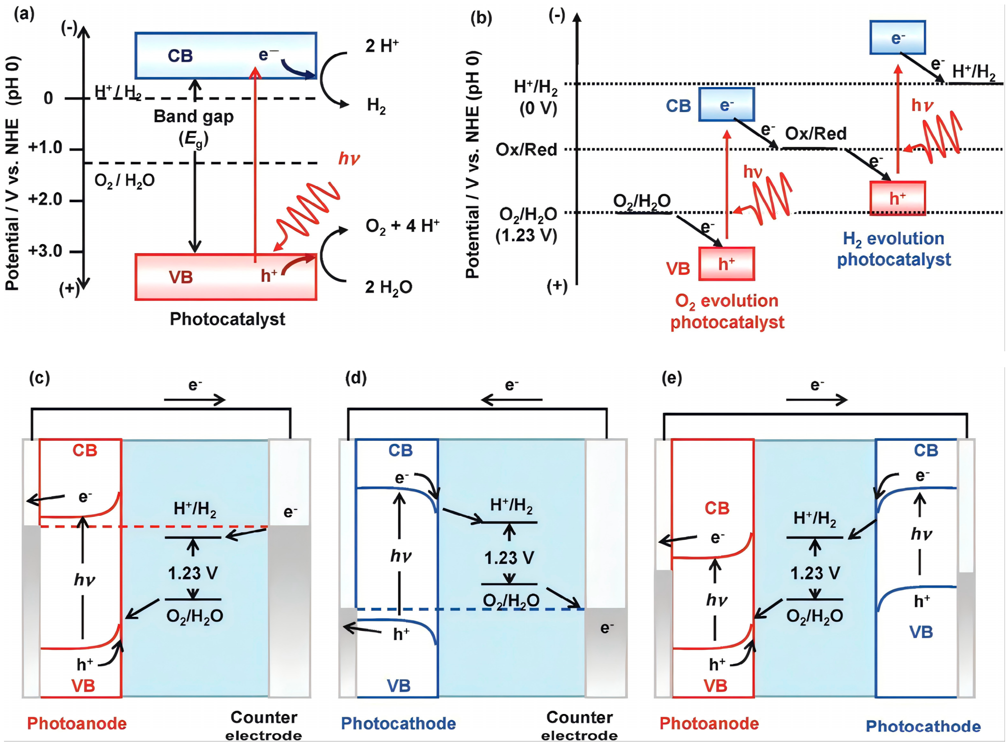

Figure 10. Schematic illustration of photocatalytic and photoelectrochemical water splitting systems. (a) Single semiconductor photocatalyst for overall water splitting. (b) Dual photocatalyst (Z-scheme) configuration using separate O_2 and H_2 evolution catalysts. (c–e) PEC water splitting configurations using photoanodes, photocathodes, and dual-photoelectrode systems, respectively[115]. Copyright, 2014 Chemical Society Reviews.

In a study, a TiO_2 PEC system was employed for the dual purpose of alcohol oxidation and hydrogen generation, achieving Faradaic efficiencies of 92% for aldehyde formation and 95% for H_2 evolution under UV light and 0.6 V bias [116]. This dual-function platform demonstrates the feasibility of coupling selective organic transformations with clean energy production.

TiO_2-based photoelectrocatalysis represents a versatile platform that integrates pollutant degradation with energy conversion. Through rational material design and system-level integration, significant advancements have been achieved in contaminant removal, pathogen inactivation, and solar-to-chemical energy transformation. Nevertheless, further work is required to address challenges related to selectivity, long-term stability, and scale-up for real-world applications—issues that will be explored in the following section.

5. Challenges and Future Prospects

5.1. Efficiency and Visible Light Utilization

TiO_2's intrinsic wide bandgap (3.0–3.2 eV) restricts its photoresponse to the UV spectrum, which accounts for less than 5% of solar radiation. Although doping, heterojunction construction, and surface plasmon resonance (SPR) have broadened its visible light activity, the overall solar-to-chemical conversion efficiency remains relatively low [117].

Future efforts should focus on constructing multi-component hybrid systems with optimized band alignments and interfacial engineering to facilitate visible light harvesting and charge transport. The integration of PEC systems with renewable electricity sources (e.g., solar PV, hydro, wind) to power the external bias represents a practical route to enhance sustainability and reduce fossil energy dependence.

5.2. Charge Separation, Transport, and Stability

While external bias improves charge separation, electron–hole recombination and low intrinsic conductivity remain major bottlenecks [118]. Tailoring electrode morphology—such as constructing 1D or 3D nanostructures—and incorporating conductive components like graphene or carbon nanotubes has shown promise [119]. Future research should explore advanced junction architectures (e.g., p–n–p or n–p–n systems) and core–shell designs to further suppress recombination while maintaining durability under operational stress [120].

5.3. Reactor Design and Scale-Up

Most PEC systems remain confined to lab-scale due to limitations in reactor design, light penetration, and electrode fabrication. Flow maldistribution and high energy input for mixing further constrain performance [2]. Novel reactor configurations—such as microfluidic and membrane-based designs—and modular, scalable systems using embroidered or roll-to-roll flexible electrodes show great potential [121]. Coupling computational fluid dynamics (CFD) modeling with experimental optimization will be critical for system-level scale-up.

6. Conclusions

This review summarizes recent advancements in TiO_2-based photoelectrocatalysis (PEC) , with an emphasis on enhancing visible light utilization and its environmental applications. The integration of photocatalysis with electrochemical bias effectively mitigates electron–hole recombination, improving charge carrier dynamics and catalytic efficiency. Spatially separated redox reactions at the photoanode and cathode enable efficient pollutant degradation and concurrent resource recovery.

Modification strategies, including doping, defect engineering, heterojunctions, and surface plasmon resonance (SPR) , have significantly improved TiO_2's performance by modulating its electronic structure and broadening its absorption spectrum. PEC systems have shown remarkable versatility in the degradation of organic pollutants, heavy metals, and in microbial disinfection, while also facilitating CO_2 reduction and hydrogen evolution.

However, challenges persist, notably in achieving high solar-to-chemical conversion efficiency, enhancing charge separation, ensuring long-term stability, and scaling up PEC reactors. Future research should focus on optimizing composite materials, reactor design, and integrating renewable energy sources, alongside employing advanced characterization and computational models to drive PEC technology toward practical industrial applications.

Author Contributions: Conceptualization, Xiongwei Liang and Shaopeng Yu; Methodology, Xiongwei Liang; Software, Xiongwei Liang; Validation, Xiongwei Liang, Shaopeng Yu, and Bo Meng; Formal Analysis, Xiongwei Liang; Investigation, Xiongwei Liang; Resources, Xiongwei Liang; Data Curation, Xiongwei Liang; Writing—Original Draft Preparation, Xiongwei Liang; Writing—Review and Editing, Xiongwei Liang, Shaopeng Yu, Bo Meng, Xiaodi Wang, Chunxue Yang, Chuanqi Shi, and Junnan Ding; Visualization, Xiongwei Liang; Supervision, Shaopeng Yu; Project Administration, Shaopeng Yu; Funding Acquisition, Shaopeng Yu. All authors have read and agreed to the published version of the manuscript.

Funding: This article was funded by the Heilongjiang Provincial Natural Science Foundation of China (LH2021E096, LH2023D015 and LH2023C066) . Harbin City Science and Technology Plan Self-ra Project (ZC2023ZJ001004)

Data Availability Statement: Data are available through request to the corresponding author.

Conflicts of Interest: The authors declare no conflicts of interest.

References

1. Li, L.; Xu, H.; Zhang, Q.; Zhan, Z.; Liang, X.; Xing, J. Estimation methods of wetland carbon sink and factors influencing wetland carbon cycle: a review. *Carbon Research* **2024**, *3*, 50, doi:10.1007/s44246-024-00135-y.

2. Brillas, E.; Garcia-Segura, S. Recent progress of applied TiO2 photoelectrocatalysis for the degradation of organic pollutants in wastewaters. *Journal of Environmental Chemical Engineering* **2023**, *11*, 109635, doi:https://doi.org/10.1016/j.jece.2023.109635.
3. Alulema-Pullupaxi, P.; Espinoza-Montero, P.J.; Sigcha-Pallo, C.; Vargas, R.; Fernández, L.; Peralta-Hernández, J.M.; Paz, J.L. Fundamentals and applications of photoelectrocatalysis as an efficient process to remove pollutants from water: A review. *Chemosphere* **2021**, *281*, 130821, doi:https://doi.org/10.1016/j.chemosphere.2021.130821.
4. Wang, J.L.; and Xu, L.J. Advanced Oxidation Processes for Wastewater Treatment: Formation of Hydroxyl Radical and Application. *Critical Reviews in Environmental Science and Technology* **2012**, *42*, 251-325, doi:10.1080/10643389.2010.507698.
5. Sirés, I.; Brillas, E.; Oturan, M.A.; Rodrigo, M.A.; Panizza, M. Electrochemical advanced oxidation processes: today and tomorrow. A review. *Environmental Science and Pollution Research* **2014**, *21*, 8336-8367, doi:10.1007/s11356-014-2783-1.
6. Li, L.; Liang, T.; Zhao, M.; Lv, Y.; Song, Z.; Sheng, T.; Ma, F. A review on mycelial pellets as biological carriers: Wastewater treatment and recovery for resource and energy. *Bioresource Technology* **2022**, *355*, 127200, doi:https://doi.org/10.1016/j.biortech.2022.127200.
7. Wang, L.; Huang, X.; Ma, F.; Ho, S.H.; Wu, J.; Zhu, S. Role of Rhizophagus irregularis in alleviating cadmium toxicity via improving the growth, micro- and macroelements uptake in Phragmites australis. *Environ Sci Pollut Res Int* **2017**, *24*, 3593-3607, doi:10.1007/s11356-016-7984-3.
8. Bai, S.; Zhu, S.; Jin, C.; Sun, Z.; Wang, L.; Wen, Q.; Ma, F. Sorption mechanisms of antibiotic sulfamethazine (SMT) on magnetite-coated biochar: pH-dependence and redox transformation. *Chemosphere* **2021**, *268*, 128805, doi:10.1016/j.chemosphere.2020.128805.
9. Li, L.; Han, J.; Huang, L.; Liu, L.; Qiu, S.; Ding, J.; Liu, X.; Zhang, J. Activation of PMS by MIL-53 (Fe) @AC composites contributes to tetracycline degradation: Properties and mechanisms. *Surfaces and Interfaces* **2024**, *51*, 104521, doi:https://doi.org/10.1016/j.surfin.2024.104521.
10. Zhang, C.; Zhou, M.; Zhang, Y.; Li, D.; Hou, N.; Zhao, X. Novel strategies for enhancing energy metabolism and wastewater treatment in algae-bacteria symbiotic system through carbon dots-induced photogenerated electrons: The definitive role of accelerated electron transport. *Chemical Engineering Journal* **2024**, *500*, 157016, doi:https://doi.org/10.1016/j.cej.2024.157016.
11. Zhao, X.; Guo, M.; Wang, Y.; Jin, M.; Hou, N.; Wu, H. Toxic effects of nanoplastics on biological nitrogen removal in constructed wetlands: Evidence from iron utilization and metabolism. *Water Research* **2024**, *256*, 121577, doi:https://doi.org/10.1016/j.watres.2024.121577.
12. Li, L.; Chai, W.; Kang, J.; Liu, J.; Xing, J.; Li, G.; Zhan, Z. Utilization of graphite tailings and coal gangue in the preparation of foamed ceramics. *International Journal of Applied Ceramic Technology* **2025**, *22*, e15012, doi:https://doi.org/10.1111/ijac.15012.
13. Zhao, X.; Meng, X.; Li, Q.; Ho, S.-H. Nitrogen metabolic responses of non-rhizosphere and rhizosphere microbial communities in constructed wetlands under nanoplastics disturbance. *Journal of Hazardous Materials* **2025**, *484*, 136777, doi:https://doi.org/10.1016/j.jhazmat.2024.136777.
14. Byrne, C.; Subramanian, G.; Pillai, S.C. Recent advances in photocatalysis for environmental applications. *Journal of Environmental Chemical Engineering* **2018**, *6*, 3531-3555, doi:https://doi.org/10.1016/j.jece.2017.07.080.
15. Huang, X.; Wang, L.; Ma, F. Arbuscular mycorrhizal fungus modulates the phytotoxicity of Cd via combined responses of enzymes, thiolic compounds, and essential elements in the roots of Phragmites australis. *Chemosphere* **2017**, *187*, 221-229, doi:10.1016/j.chemosphere.2017.08.021.
16. Liu, M.; Li, N.; Meng, S.; Yang, S.; Jing, B.; Zhang, J.; Jiang, J.; Qiu, S.; Deng, F. Bio-inspired Cu2O cathode for O2 capturing and oxidation boosting in electro-Fenton for sulfathiazole decay. *Journal of Hazardous Materials* **2024**, *478*, 135484, doi:https://doi.org/10.1016/j.jhazmat.2024.135484.
17. Hou, Y.; Zuo, F.; Dagg, A.; Feng, P. Visible Light-Driven α-Fe2O3 Nanorod/Graphene/BiV1–xMoxO4 Core/Shell Heterojunction Array for Efficient Photoelectrochemical Water Splitting. *Nano Letters* **2012**, *12*, 6464-6473, doi:10.1021/nl303961c.

18. Zheng, Y.; Lin, L.; Wang, B.; Wang, X. Graphitic Carbon Nitride Polymers toward Sustainable Photoredox Catalysis. *Angew Chem Int Ed Engl* **2015**, *54*, 12868-12884, doi:10.1002/anie.201501788.
19. Zhang, G.; Lan, Z.-A.; Wang, X. Conjugated Polymers: Catalysts for Photocatalytic Hydrogen Evolution. *Angewandte Chemie International Edition* **2016**, *55*, 15712-15727, doi:https://doi.org/10.1002/anie.201607375.
20. Wang, J.; Chen, H. Catalytic ozonation for water and wastewater treatment: Recent advances and perspective. *Science of The Total Environment* **2020**, *704*, 135249, doi:https://doi.org/10.1016/j.scitotenv.2019.135249.
21. Fujishima, A.; Honda, K. Electrochemical Photolysis of Water at a Semiconductor Electrode. *Nature* **1972**, *238*, 37-38, doi:10.1038/238037a0.
22. Schneider, J.; Matsuoka, M.; Takeuchi, M.; Zhang, J.; Horiuchi, Y.; Anpo, M.; Bahnemann, D.W. Understanding TiO2 Photocatalysis: Mechanisms and Materials. *Chemical Reviews* **2014**, *114*, 9919-9986, doi:10.1021/cr5001892.
23. Pelaez, M.; Nolan, N.T.; Pillai, S.C.; Seery, M.K.; Falaras, P.; Kontos, A.G.; Dunlop, P.S.M.; Hamilton, J.W.J.; Byrne, J.A.; O'Shea, K.; et al. A review on the visible light active titanium dioxide photocatalysts for environmental applications. *Applied Catalysis B: Environmental* **2012**, *125*, 331-349, doi:https://doi.org/10.1016/j.apcatb.2012.05.036.
24. Daghrir, R.; Drogui, P.; Robert, D. Modified TiO2 For Environmental Photocatalytic Applications: A Review. *Industrial & Engineering Chemistry Research* **2013**, *52*, 3581-3599, doi:10.1021/ie303468t.
25. Nakata, K.; Fujishima, A. TiO2 photocatalysis: Design and applications. *Journal of Photochemistry and Photobiology C: Photochemistry Reviews* **2012**, *13*, 169-189, doi:https://doi.org/10.1016/j.jphotochemrev.2012.06.001.
26. Chen, X.; Mao, S.S. Titanium Dioxide Nanomaterials: Synthesis, Properties, Modifications, and Applications. *Chemical Reviews* **2007**, *107*, 2891-2959, doi:10.1021/cr0500535.
27. Hoffmann, M.R.; Martin, S.T.; Choi, W.; Bahnemann, D.W. Environmental Applications of Semiconductor Photocatalysis. *Chemical Reviews* **1995**, *95*, 69-96, doi:10.1021/cr00033a004.
28. Linsebigler, A.L.; Lu, G.; Yates, J.T., Jr. Photocatalysis on TiO2 Surfaces: Principles, Mechanisms, and Selected Results. *Chemical Reviews* **1995**, *95*, 735-758, doi:10.1021/cr00035a013.
29. Asahi, R.; Morikawa, T.; Ohwaki, T.; Aoki, K.; Taga, Y. Visible-Light Photocatalysis in Nitrogen-Doped Titanium Oxides. *Science* **2001**, *293*, 269-271, doi:doi:10.1126/science.1061051.
30. Chen, X.; Liu, L.; Yu, P.Y.; Mao, S.S. Increasing Solar Absorption for Photocatalysis with Black Hydrogenated Titanium Dioxide Nanocrystals. *Science* **2011**, *331*, 746-750, doi:doi:10.1126/science.1200448.
31. Wang, H.; Zhang, L.; Chen, Z.; Hu, J.; Li, S.; Wang, Z.; Liu, J.; Wang, X. Semiconductor heterojunction photocatalysts: design, construction, and photocatalytic performances. *Chemical Society Reviews* **2014**, *43*, 5234-5244, doi:10.1039/C4CS00126E.
32. Linic, S.; Christopher, P.; Ingram, D.B. Plasmonic-metal nanostructures for efficient conversion of solar to chemical energy. *Nature Materials* **2011**, *10*, 911-921, doi:10.1038/nmat3151.
33. Ong, W.-J.; Tan, L.-L.; Ng, Y.H.; Yong, S.-T.; Chai, S.-P. Graphitic Carbon Nitride (g-C3N4) -Based Photocatalysts for Artificial Photosynthesis and Environmental Remediation: Are We a Step Closer To Achieving Sustainability? *Chemical Reviews* **2016**, *116*, 7159-7329, doi:10.1021/acs.chemrev.6b00075.
34. Jiang, L.; Yuan, X.; Zeng, G.; Liang, J.; Chen, X.; Yu, H.; Wang, H.; Wu, Z.; Zhang, J.; Xiong, T. In-situ synthesis of direct solid-state dual Z-scheme WO3/g-C3N4/Bi2O3 photocatalyst for the degradation of refractory pollutant. *Applied Catalysis B: Environmental* **2018**, *227*, 376-385, doi:https://doi.org/10.1016/j.apcatb.2018.01.042.
35. Garcia-Segura, S.; Brillas, E. Applied photoelectrocatalysis on the degradation of organic pollutants in wastewaters. *Journal of Photochemistry and Photobiology C: Photochemistry Reviews* **2017**, *31*, 1-35, doi:https://doi.org/10.1016/j.jphotochemrev.2017.01.005.
36. Boldrin Zanoni, M.V.; Guaraldo, T.T.; Garcia Bessegato, G. Enhancement of Photoelectrocatalysis Efficiency by Using Nanostructured Electrodes. In *Modern Electrochemical Methods in Nano, Surface and Corrosion Science*, Aliofkhazraei, M., Ed.; IntechOpen: Rijeka, 2014.

37. Zarei, E.; Ojani, R. Fundamentals and some applications of photoelectrocatalysis and effective factors on its efficiency: a review. *Journal of Solid State Electrochemistry* **2017**, *21*, 305-336, doi:10.1007/s10008-016-3385-2.
38. Martínez-Huitle, C.A.; Brillas, E. Decontamination of wastewaters containing synthetic organic dyes by electrochemical methods: A general review. *Applied Catalysis B: Environmental* **2009**, *87*, 105-145, doi:https://doi.org/10.1016/j.apcatb.2008.09.017.
39. Panizza, M.; Cerisola, G. Direct And Mediated Anodic Oxidation of Organic Pollutants. *Chemical Reviews* **2009**, *109*, 6541-6569, doi:10.1021/cr9001319.
40. Moreira, F.C.; Boaventura, R.A.R.; Brillas, E.; Vilar, V.J.P. Electrochemical advanced oxidation processes: A review on their application to synthetic and real wastewaters. *Applied Catalysis B: Environmental* **2017**, *202*, 217-261, doi:https://doi.org/10.1016/j.apcatb.2016.08.037.
41. Bessegato, G.G.; Guaraldo, T.T.; de Brito, J.F.; Brugnera, M.F.; Zanoni, M.V.B. Achievements and Trends in Photoelectrocatalysis: from Environmental to Energy Applications. *Electrocatalysis* **2015**, *6*, 415-441, doi:10.1007/s12678-015-0259-9.
42. Daghrir, R.; Drogui, P.; Robert, D. Photoelectrocatalytic technologies for environmental applications. *Journal of Photochemistry and Photobiology A: Chemistry* **2012**, *238*, 41-52, doi:https://doi.org/10.1016/j.jphotochem.2012.04.009.
43. Cheng, X.; Cheng, Q.; Deng, X.; Wang, P.; Liu, H. A facile and novel strategy to synthesize reduced TiO2 nanotubes photoelectrode for photoelectrocatalytic degradation of diclofenac. *Chemosphere* **2016**, *144*, 888-894, doi:https://doi.org/10.1016/j.chemosphere.2015.09.070.
44. Fujishima, A.; Rao, T.N.; Tryk, D.A. Titanium dioxide photocatalysis. *Journal of Photochemistry and Photobiology C: Photochemistry Reviews* **2000**, *1*, 1-21, doi:https://doi.org/10.1016/S1389-5567 (00) 00002-2.
45. Hashimoto, K.; Irie, H.; Fujishima, A. TiO2 Photocatalysis: A Historical Overview and Future Prospects. *Japanese Journal of Applied Physics* **2005**, *44*, 8269, doi:10.1143/JJAP.44.8269.
46. Vinodgopal, K.; Hotchandani, S.; Kamat, P.V. Electrochemically assisted photocatalysis: titania particulate film electrodes for photocatalytic degradation of 4-chlorophenol. *The Journal of Physical Chemistry* **1993**, *97*, 9040-9044, doi:10.1021/j100137a033.
47. Jiang, D.; Zhao, H.; Zhang, S.; John, R. Kinetic study of photocatalytic oxidation of adsorbed carboxylic acids at TiO2 porous films by photoelectrolysis. *Journal of Catalysis* **2004**, *223*, 212-220, doi:https://doi.org/10.1016/j.jcat.2004.01.030.
48. Grätzel, M. Photoelectrochemical cells. *Nature* **2001**, *414*, 338-344, doi:10.1038/35104607.
49. Kudo, A.; Miseki, Y. Heterogeneous photocatalyst materials for water splitting. *Chemical Society Reviews* **2009**, *38*, 253-278, doi:10.1039/B800489G.
50. Liao, C.-H.; Huang, C.-W.; Wu, J.C.S. Hydrogen Production from Semiconductor-based Photocatalysis via Water Splitting. *Catalysts* **2012**, *2*, 490-516.
51. Abe, R. Recent progress on photocatalytic and photoelectrochemical water splitting under visible light irradiation. *Journal of Photochemistry and Photobiology C: Photochemistry Reviews* **2010**, *11*, 179-209, doi:https://doi.org/10.1016/j.jphotochemrev.2011.02.003.
52. Luttrell, T.; Halpegamage, S.; Tao, J.; Kramer, A.; Sutter, E.; Batzill, M. Why is anatase a better photocatalyst than rutile? - Model studies on epitaxial TiO2 films. *Scientific Reports* **2014**, *4*, 4043, doi:10.1038/srep04043.
53. Scanlon, D.O.; Dunnill, C.W.; Buckeridge, J.; Shevlin, S.A.; Logsdail, A.J.; Woodley, S.M.; Catlow, C.R.A.; Powell, M.J.; Palgrave, R.G.; Parkin, I.P.; et al. Band alignment of rutile and anatase TiO2. *Nature Materials* **2013**, *12*, 798-801, doi:10.1038/nmat3697.
54. Jiang, X.; Zhang, Y.; Jiang, J.; Rong, Y.; Wang, Y.; Wu, Y.; Pan, C. Characterization of Oxygen Vacancy Associates within Hydrogenated TiO2: A Positron Annihilation Study. *The Journal of Physical Chemistry C* **2012**, *116*, 22619-22624, doi:10.1021/jp307573c.
55. Liu, N.; Schneider, C.; Freitag, D.; Hartmann, M.; Venkatesan, U.; Müller, J.; Spiecker, E.; Schmuki, P. Black TiO2 Nanotubes: Cocatalyst-Free Open-Circuit Hydrogen Generation. *Nano Letters* **2014**, *14*, 3309-3313, doi:10.1021/nl500710j.

56. Wang, G.; Wang, H.; Ling, Y.; Tang, Y.; Yang, X.; Fitzmorris, R.C.; Wang, C.; Zhang, J.Z.; Li, Y. Hydrogen-Treated TiO2 Nanowire Arrays for Photoelectrochemical Water Splitting. *Nano Letters* **2011**, *11*, 3026-3033, doi:10.1021/nl201766h.
57. Nah, Y.-C.; Paramasivam, I.; Schmuki, P. Doped TiO2 and TiO2 Nanotubes: Synthesis and Applications. *ChemPhysChem* **2010**, *11*, 2698-2713, doi:https://doi.org/10.1002/cphc.201000276.
58. Sakata, K.; Amemiya, K. Real-time and operando observation of intermediates on TiO2 photoelectrocatalysis by soft X-ray absorption spectroscopy. *Electrochemistry Communications* **2024**, *165*, 107771, doi:https://doi.org/10.1016/j.elecom.2024.107771.
59. Tamaki, Y.; Furube, A.; Murai, M.; Hara, K.; Katoh, R.; Tachiya, M. Dynamics of efficient electron–hole separation in TiO2 nanoparticles revealed by femtosecond transient absorption spectroscopy under the weak-excitation condition. *Physical Chemistry Chemical Physics* **2007**, *9*, 1453-1460, doi:10.1039/B617552J.
60. Yamakata, A.; Ishibashi, T.-a.; Onishi, H. Time-resolved infrared absorption spectroscopy of photogenerated electrons in platinized TiO2 particles. *Chemical Physics Letters* **2001**, *333*, 271-277, doi:https://doi.org/10.1016/S0009-2614 (00) 01374-9.
61. Nosaka, Y.; Nosaka, A.Y. Generation and Detection of Reactive Oxygen Species in Photocatalysis. *Chemical Reviews* **2017**, *117*, 11302-11336, doi:10.1021/acs.chemrev.7b00161.
62. Ishibashi, K.-i.; Fujishima, A.; Watanabe, T.; Hashimoto, K. Quantum yields of active oxidative species formed on TiO2 photocatalyst. *Journal of Photochemistry and Photobiology A: Chemistry* **2000**, *134*, 139-142, doi:https://doi.org/10.1016/S1010-6030 (00) 00264-1.
63. Buxton, G.V.; Greenstock, C.L.; Helman, W.P.; Ross, A.B. Critical Review of rate constants for reactions of hydrated electrons, hydrogen atoms and hydroxyl radicals (·OH/·O− in Aqueous Solution. *Journal of Physical and Chemical Reference Data* **1988**, *17*, 513-886, doi:10.1063/1.555805 %J Journal of Physical and Chemical Reference Data.
64. Gligorovski, S.; Strekowski, R.; Barbati, S.; Vione, D. Environmental Implications of Hydroxyl Radicals (•OH) . *Chemical Reviews* **2015**, *115*, 13051-13092, doi:10.1021/cr500310b.
65. Fujishima, A.; Zhang, X.; Tryk, D.A. TiO2 photocatalysis and related surface phenomena. *Surface Science Reports* **2008**, *63*, 515-582, doi:https://doi.org/10.1016/j.surfrep.2008.10.001.
66. Hirakawa, T.; Nosaka, Y. Properties of O2 •- and OH• Formed in TiO2 Aqueous Suspensions by Photocatalytic Reaction and the Influence of H2O2 and Some Ions. *Langmuir* **2002**, *18*, 3247-3254, doi:10.1021/la015685a.
67. Daimon, T.; Nosaka, Y. Formation and Behavior of Singlet Molecular Oxygen in TiO2 Photocatalysis Studied by Detection of Near-Infrared Phosphorescence. *The Journal of Physical Chemistry C* **2007**, *111*, 4420-4424, doi:10.1021/jp070028y.
68. Turchi, C.S.; Ollis, D.F. Photocatalytic degradation of organic water contaminants: Mechanisms involving hydroxyl radical attack. *Journal of Catalysis* **1990**, *122*, 178-192, doi:https://doi.org/10.1016/0021-9517 (90) 90269-P.
69. Ollis, D.F. Kinetics of Liquid Phase Photocatalyzed Reactions: An Illuminating Approach. *The Journal of Physical Chemistry B* **2005**, *109*, 2439-2444, doi:10.1021/jp040236f.
70. Ju, L.; Wu, P.; Ju, Y.; Chen, M.; Yang, S.; Zhu, H. The degradation mechanism of Bisphenol A by photoelectrocatalysis using new materials as the working electrode. *Surfaces and Interfaces* **2021**, *23*, 100967, doi:https://doi.org/10.1016/j.surfin.2021.100967.
71. Liang, X.; Yu, S.; Meng, B.; Liu, J.; Yang, C.; Shi, C.; Ding, J. Enhanced Degradation of Carbamazepine from Constructed Wetlands with a PEC System Based on an Anode of N-TiO2 Nanocrystal-Modified TiO2 Nanotubes and an Activated Carbon Photocathode. *Separations* **2024**, *11*, 216.
72. Ohtani, B.; Prieto-Mahaney, O.O.; Li, D.; Abe, R. What is Degussa (Evonik) P25? Crystalline composition analysis, reconstruction from isolated pure particles and photocatalytic activity test. *Journal of Photochemistry and Photobiology A: Chemistry* **2010**, *216*, 179-182, doi:https://doi.org/10.1016/j.jphotochem.2010.07.024.
73. Heikkilä, M.; Puukilainen, E.; Ritala, M.; Leskelä, M. Effect of thickness of ALD grown TiO2 films on photoelectrocatalysis. *Journal of Photochemistry and Photobiology A: Chemistry* **2009**, *204*, 200-208, doi:https://doi.org/10.1016/j.jphotochem.2009.03.019.

74. Jiang, D.; Zhao, H.; Zhang, S.; John, R.; Will, G.D. Photoelectrochemical measurement of phthalic acid adsorption on porous TiO 2 film electrodes. *Journal of Photochemistry and Photobiology, A: Chemistry* **2003**, *156*, 201-206, doi:10.1016/S1010-6030 (02) 00409-4.
75. Herrmann, J.-M. Heterogeneous photocatalysis: fundamentals and applications to the removal of various types of aqueous pollutants. *Catalysis Today* **1999**, *53*, 115-129, doi:https://doi.org/10.1016/S0920-5861 (99) 00107-8.
76. Burns, R.A.; Crittenden, J.C.; Hand, D.W.; Selzer, V.H.; Sutter, L.L.; Salman, S.R. Effect of Inorganic Ions in Heterogeneous Photocatalysis of TCE. *Journal of Environmental Engineering* **1999**, *125*, 77-85, doi:doi:10.1061/ (ASCE) 0733-9372 (1999) 125:1 (77) .
77. Zaleska, A. Doped-TiO2: A Review. *Recent Patents on Engineering* **2008**, *2*, 157-164, doi:https://doi.org/10.2174/187221208786306289.
78. Liu, G.; Yin, L.C.; Wang, J.; Niu, P.; Zhen, C.; Xie, Y.; Cheng, H.M. A red anatase TiO2 photocatalyst for solar energy conversion. *Energy & Environmental Science* **2012**, *5*, 9603-9610, doi:10.1039/C2EE22930G.
79. Chen, M.; Sun, Y.-h.; Zhou, D.; Yan, Y.; Sun, L.; Cheng, H.-B.; Chen, Z.; Tang, C.-M.; Chang, L.; Xu, J.-Q. Efficient CO2 reduction to C2 products in a Ce-TiO2 photoanode-driven photoelectrocatalysis system using a Bnanometer Cu2O cathode. *Applied Catalysis A: General* **2024**, *687*, 119966, doi:https://doi.org/10.1016/j.apcata.2024.119966.
80. Lucilha, A.C.; Camargo, L.P.; Liberatti, V.R.; Barbosa, E.C.M.; Dall'Antonia, L.H. Zn1-xCoxO vs Ag-ZnO photoanodes design via combustion: Characterization and application in photoelectrocatalysis. *Colloids and Surfaces A: Physicochemical and Engineering Aspects* **2022**, *638*, 128261, doi:https://doi.org/10.1016/j.colsurfa.2022.128261.
81. Nada, A.; Orimolade, B.; El-Maghrabi, H.; Koiki, B.; Rivallin, M.; Bekheet, M.; Viter, R.; Damberga, D.; Lesage, G.; Iatsunskyi, I.; et al. Photoelectrocatalysis of paracetamol on Pd-ZnO/ N-doped carbon nanofibers electrode. *Applied Materials Today* **2021**, *24*, 101129, doi:10.1016/j.apmt.2021.101129.
82. Ihara, T.; Miyoshi, M.; Iriyama, Y.; Matsumoto, O.; Sugihara, S. Visible-light-active titanium oxide photocatalyst realized by an oxygen-deficient structure and by nitrogen doping. *Applied Catalysis B: Environmental* **2003**, *42*, 403-409, doi:https://doi.org/10.1016/S0926-3373 (02) 00269-2.
83. Yin, R.; Chen, Y.; Lu, G.; Zeng, L.; Choi, W.; Zhu, M. Complexes of Fe (III) -organic pollutants that directly activate Fenton-like processes under visible light. *Applied Catalysis B: Environmental* **2020**, *283*, 119663, doi:10.1016/j.apcatb.2020.119663.
84. Ali, M.; Anjum, A.S.; Bibi, A.; Wageh, S.; Sun, K.C.; Jeong, S.H. Gradient heating-induced bi-phase synthesis of carbon quantum dots (CQDs) on graphene-coated carbon cloth for efficient photoelectrocatalysis. *Carbon* **2022**, *196*, 649-662, doi:https://doi.org/10.1016/j.carbon.2022.05.040.
85. Li, H.; Zhang, X.; Huo, Y.; Zhu, J. Supercritical Preparation of a Highly Active S-Doped TiO 2 Photocatalyst for Methylene Blue Mineralization. *Environmental science & technology* **2007**, *41*, 4410-4414, doi:10.1021/es062680x.
86. Raizada, P.; Soni, V.; Kumar, A.; Singh, P.; Parwaz Khan, A.A.; Asiri, A.M.; Thakur, V.K.; Nguyen, V.-H. Surface defect engineering of metal oxides photocatalyst for energy application and water treatment. *Journal of Materiomics* **2021**, *7*, 388-418, doi:https://doi.org/10.1016/j.jmat.2020.10.009.
87. Li, H.; Li, M.; Jiang, B.; Liu, R.; Li, Q.; Shaik, F. Effect of 3D titanium substrates with TiO2 nanotube arrays on photoelectrocatalysis degradation of phenol. *Journal of Environmental Chemical Engineering* **2023**, *11*, 111557, doi:https://doi.org/10.1016/j.jece.2023.111557.
88. Low, J.; Yu, J.; Jaroniec, M.; Wageh, S.; Al-Ghamdi, A.A. Heterojunction Photocatalysts. *Advanced Materials* **2017**, *29*, 1601694, doi:https://doi.org/10.1002/adma.201601694.
89. Ai, M.; Peng, Z.; Li, X.; Idrees, F.; Zhang, X.; Zou, J.-J.; Pan, L. Piezoelectric-enhanced n-TiO2/BaTiO3/p-TiO2 heterojunction for highly efficient photoelectrocatalysis. *Green Energy & Environment* **2023**, doi:10.1016/j.gee.2023.12.001.
90. Yang, Z.; Zhao, L.; Zhang, S.; Zhao, X.J.A.M.T. Ferroelectric-enhanced BiVO4-BiFeO3 photoelectrocatalysis for efficient, stable and large-current-density oxygen evolution. *Applied Materials Today* **2022**.
91. Low, J.; Jiang, C.; Cheng, B.; Wageh, S.; Al-Ghamdi, A.A.; Yu, J. A Review of Direct Z-Scheme Photocatalysts. *Small Methods* **2017**, *1*, 1700080, doi:https://doi.org/10.1002/smtd.201700080.

92. Zeng, Q.-r.; Jia, Z.-a.; Liu, X.; Xiu, B.-w.; Cheng, J.-p. Multi-Interface polarization engineering constructed 1T-2H MoS2 QDs/Y-NaBi (MoO4) 2 multiple heterostructure for high-efficient piezoelectric-photoelectrocatalysis PDE-5i degradation. *Applied Catalysis B: Environmental* **2023**, *327*, 122460, doi:https://doi.org/10.1016/j.apcatb.2023.122460.
93. Leary, R.; Westwood, A. Carbonaceous nanomaterials for the enhancement of TiO2 photocatalysis. *Carbon* **2011**, *49*, 741-772, doi:https://doi.org/10.1016/j.carbon.2010.10.010.
94. Meng, X.; Zhang, Z. Two dimensional graphitic materials for photoelectrocatalysis: A short review. *Catalysis Today* **2018**, *315*, 2-8, doi:https://doi.org/10.1016/j.cattod.2018.03.015.
95. Hasan, M.R.; Hamid, S.B.A.; Basirun, W.J. Charge transfer behavior of graphene-titania photoanode in CO2 photoelectrocatalysis process. *Applied Surface Science* **2015**, *339*, 22-27, doi:https://doi.org/10.1016/j.apsusc.2015.02.162.
96. Yu, X.; Han, X.; Zhao, Z.; Zhang, J.; Guo, W.; Pan, C.; Li, A.; Liu, H.; Lin Wang, Z. Hierarchical TiO2 nanowire/graphite fiber photoelectrocatalysis setup powered by a wind-driven nanogenerator: A highly efficient photoelectrocatalytic device entirely based on renewable energy. *Nano Energy* **2015**, *11*, 19-27, doi:https://doi.org/10.1016/j.nanoen.2014.09.024.
97. Waheed, M.; Naz, G.; Ali, J.; Shoaib, M.; Arshad, M.; Baig, N.; Haidary, A.; Almoneef, M.; A. Awad, M. Plasmon-enhanced Photoelectrocatalysis by Silver/Vanadium Oxide Nanocomposites. *Optical Materials* **2025**, *160*, 116698, doi:10.1016/j.optmat.2025.116698.
98. Brongersma, M.L.; Halas, N.J.; Nordlander, P. Plasmon-induced hot carrier science and technology. *Nature Nanotechnology* **2015**, *10*, 25-34, doi:10.1038/nnano.2014.311.
99. Paramasivam, I.; Jha, H.; Liu, N.; Schmuki, P. A Review of Photocatalysis using Self-organized TiO2 Nanotubes and Other Ordered Oxide Nanostructures. *Small,* **2012**, *8*, 3073-3103, doi:https://doi.org/10.1002/smll.201200564.
100. Sboui, M.; Niu, W.; Li, D.; Lu, G.; Zhou, N.; Zhang, K.; Pan, J.H. Fabrication of electrically conductive TiO2/PANI/PVDF composite membranes for simultaneous photoelectrocatalysis and microfiltration of azo dye from wastewater. *Applied Catalysis A: General* **2022**, *644*, 118837, doi:https://doi.org/10.1016/j.apcata.2022.118837.
101. An, P.; Lv, Y.; Xiu, H.; Chen, J.; Ren, P.; Bai, Y.; Tao, C.; Ao, C.; Yang, C.; Wu, J.; et al. Triboelectric-electromagnetic nanogenerator coupled type-II heterojunction enhancing photoelectrocatalysis for wastewater degradation. *Nano Energy* **2025**, *134*, 110589, doi:https://doi.org/10.1016/j.nanoen.2024.110589.
102. Brillas, E.; Manuel Peralta-Hernández, J. Removal of paracetamol (acetaminophen) by photocatalysis and photoelectrocatalysis. A critical review. *Separation and Purification Technology* **2023**, *309*, 122982, doi:https://doi.org/10.1016/j.seppur.2022.122982.
103. Fernandes, C.H.M.; Goulart, L.A.; Gonçalves, R.; Santos, G.O.S.; Zanoni, M.V.B.; Mascaro, L.H.; Lanza, M.R.V. Effective photoelectrocatalysis of levofloxacin antibiotic with Ti/IrO2Nb2O5 in environmental samples. *Electrochimica Acta* **2024**, *475*, 143586, doi:https://doi.org/10.1016/j.electacta.2023.143586.
104. Barbosa, M.L.; Costa, M.J.S.; Lima, A.E.B.; Batista, A.M.; Longo, E.; Cavalcante, L.S.; Santos, R.S. Anionic and cationic dyes removal by degradation via photoelectrocatalysis using a WO3/CuWO4 heterojunction film as a photoanode. *Nano-Structures & Nano-Objects* **2023**, *35*, 100993, doi:10.1016/j.nanoso.2023.100993.
105. Fernández-Domene, R.M.; Sánchez-Tovar, R.; Lucas-granados, B.; Muñoz-Portero, M.J.; García-Antón, J. Elimination of pesticide atrazine by photoelectrocatalysis using a photoanode based on WO3 nanosheets. *Chemical Engineering Journal* **2018**, *350*, 1114-1124, doi:https://doi.org/10.1016/j.cej.2018.06.015.
106. Zhang, Y.; Xu, X.; Cai, J.; Pan, Y.; Zhou, M. Degradation of 2,4-dichlorophenoxyacetic acid by a novel photoelectrocatalysis/photoelectro-Fenton process using Blue-TiO2 nanotube arrays as the anode. *Chemosphere* **2021**, *266*, 129063, doi:https://doi.org/10.1016/j.chemosphere.2020.129063.
107. Li, D.; Jia, J.; Zhang, Y.; Wang, N.; Guo, X.; Yu, X. Preparation and characterization of Nano-graphite/TiO2 composite photoelectrode for photoelectrocatalytic degradation of hazardous pollutant. *Journal of Hazardous Materials* **2016**, *315*, 1-10, doi:https://doi.org/10.1016/j.jhazmat.2016.04.053.
108. Ma, B.; Xin, S.; Liu, W.; She, Z.; Zhao, Y.; Guo, L.; Jin, C.; Ji, J.; Gao, M. Synergic removal of p-chloronitrobenzene by reduced graphene oxide/BiOBr/TiO2 nanotube arrays photoelectrocatalysis

coupled biodegradation: Performance and microbial response. *Journal of Water Process Engineering* **2022**, *49*, 103008, doi:https://doi.org/10.1016/j.jwpe.2022.103008.

109. Zhao, Y.; Chang, W.; Huang, Z.; Feng, X.; Ma, L.; Qi, X.; Li, Z. Enhanced removal of toxic Cr (VI) in tannery wastewater by photoelectrocatalysis with synthetic TiO2 hollow spheres. *Applied Surface Science* **2017**, *405*, 102-110, doi:https://doi.org/10.1016/j.apsusc.2017.01.306.
110. Wei, X.-P.; Ni, H.-G. The catalytic role of Cr (VI) in promoting the degradation of organic pollutants via TiO2/SnO2/BiVO4 photoelectrocatalysis: As an electron transfer carrier. *Environmental Pollution* **2025**, *366*, 125543, doi:https://doi.org/10.1016/j.envpol.2024.125543.
111. Ye, S.; Chen, Y.; Yao, X.; Zhang, J. Simultaneous removal of organic pollutants and heavy metals in wastewater by photoelectrocatalysis: A review. *Chemosphere* **2021**, *273*, 128503, doi:https://doi.org/10.1016/j.chemosphere.2020.128503.
112. Wang, Z.; He, H.; Zhao, J.; Jian, X.; Liu, C.; Gao Supervison, Z.; Song, Y.-Y. Enhanced inactivation of bacteria on capacitive semiconductor nanotubes by Self-Discharging triggered photoelectrocatalysis. *Applied Surface Science* **2023**, *611*, 155660, doi:https://doi.org/10.1016/j.apsusc.2022.155660.
113. Ebadi, S.; Ghasemipanah, K.; Alaie, E.; Rashidi, A.; Khataee, A. COD removal from gasfield produced water using photoelectrocatalysis process on coil type microreactor. *Journal of Industrial and Engineering Chemistry* **2021**, *98*, 262-269, doi:https://doi.org/10.1016/j.jiec.2021.03.045.
114. Yang, H.; Gao, F.; Zhou, W.; Gao, N.; Zhang, D.; Li, Z.; Nan, C. Efficient CO2 reduction to formate in a photoanode-driven photoelectrocatalysis system using a Bi2Se3/Bi2O3 nanocomposite cathode. *Applied Surface Science* **2023**, *623*, 157097, doi:https://doi.org/10.1016/j.apsusc.2023.157097.
115. Hisatomi, T.; Kubota, J.; Domen, K. Recent advances in semiconductors for photocatalytic and photoelectrochemical water splitting. *Chemical Society Reviews* **2014**, *43*, 7520-7535.
116. Miao, Y.; Shao, M. Photoelectrocatalysis for high-value-added chemicals production. *Chinese Journal of Catalysis* **2022**, *43*, 595-610, doi:https://doi.org/10.1016/S1872-2067 (21) 63923-2.
117. Cifre-Herrando, M.; Roselló-Márquez, G.; García-Antón, J. Is photoelectrocatalysis an efficient process to degrade endocrine disruptors chemicals? *Environmental Toxicology and Pharmacology* **2024**, *107*, 104420, doi:https://doi.org/10.1016/j.etap.2024.104420.
118. Dang, Q.; Wang, L.; Liu, J.; Wang, D.; Chai, J.; Wu, M.; Tang, L. Recent progress of photoelectrocatalysis systems for wastewater treatment. *Journal of Water Process Engineering* **2023**, *53*, 103609, doi:https://doi.org/10.1016/j.jwpe.2023.103609.
119. Wang, Y.; Zu, M.; Zhou, X.; Lin, H.; Peng, F.; Zhang, S. Designing efficient TiO2-based photoelectrocatalysis systems for chemical engineering and sensing. *Chemical Engineering Journal* **2019**, *381*, 122605, doi:10.1016/j.cej.2019.122605.
120. Xie, J.; Wang, S.; Lu, T.; Yang, S.; Zou, L.; Ren, J.; Lu, X.; Huang, J.; Huang, C.; Yang, P.J.J.o.c.; et al. Evaluating high temperature photoelectrocatalysis of TiO2 model photoanode. *Journal of colloid and interface science* **2023**, *645*, 765-774.
121. Yin, C.; Ba, L. Large-scale mechanically automated embroidered flexible electronic fabrics photoelectrocatalysis degradation of the interior air pollutant formaldehyde. *Journal of Environmental Chemical Engineering* **2024**, *12*, 112192, doi:10.1016/j.jece.2024.112192.